

PAPER

Electric field determination in air plasmas from intensity ratio of nitrogen spectral bands: I. Sensitivity analysis and uncertainty quantification of dominant processes

To cite this article: Adam Obrusník *et al* 2018 *Plasma Sources Sci. Technol.* **27** 085013

View the [article online](#) for updates and enhancements.

You may also like

- [Properties and characteristics of the nanosecond discharge developing at the water–air interface: tracking evolution from a diffused streamer to a spark filament](#)
Garima Arora, Petr Hoffer, Václav Prukner et al.

- [Foundations of plasma standards](#)
Luís L Alves, Markus M Becker, Jan van Dijk et al.

- [Uncertainty quantification and propagation in CALPHAD modeling](#)
Pejman Honarmandi, Noah H Paulson, Raymundo Arróyave et al.

HIDEN ANALYTICAL

Analysis Solutions for your **Plasma Research**

The advertisement features the Hiden Analytical logo at the top left. To the right, the text "Analysis Solutions for your **Plasma Research**" is displayed. Below this, there are four main sections with images and text:

- Surface Science**: Shows a person in blue gloves holding a small electronic component. Below it, a list includes "Surface Analysis", "SIMS", "3D depth Profiling", and "Nanometre depth resolution".
- Plasma Diagnostics**: Shows a cluster of probe tips. Below it, a list includes "Plasma characterisation", "Customised systems to suit plasma Configuration", "Mass and energy analysis of plasma ions", and "Characterisation of neutrals and radicals".
- Knowledge**, **Experience**, **Expertise**: A list of three bullet points.
- Click to view our product catalogue**: A button to access the catalogue.

Contact Hiden Analytical for further details:
W www.HidenAnalytical.com
E info@hiden.co.uk

Electric field determination in air plasmas from intensity ratio of nitrogen spectral bands: I. Sensitivity analysis and uncertainty quantification of dominant processes

Adam Obrusník^{1,3} , Petr Bílek^{1,3} , Tomáš Hoder¹, Milan Šimek²  and Zdeněk Bonaventura¹ 

¹ Department of Physical Electronics, Faculty of Science, Masaryk University, Kotlářská 2, 611 37 Brno, Czech Republic

² Department of Pulse Plasma Systems, Institute of Plasma Physics, Academy of Sciences of the Czech Republic, Prague, Czech Republic

E-mail: adam.obrusnik@gmail.com and petrbilek248@gmail.com

Received 28 March 2018, revised 19 July 2018

Accepted for publication 27 July 2018

Published 28 August 2018



Abstract

The ratio of the spectral band intensities of the first negative and second positive spectral systems of molecular nitrogen is a well recognized method for indirect determination of the electric field. It is applied for various plasmas, e.g. barrier and corona discharges for industrial applications or geophysical plasmas occurring in the Earth's atmosphere. The method relies on the dependence of the intensity ratio $R(E/N)$ of selected bands on the reduced electric field strength. Both experimental and theoretical approaches have been used to determine this dependence, yet there still is a rather large spread in the data available in literature. The primary aim of this work is to quantify the overall uncertainty of the theoretical $R(E/N)$ dependence and identify the main sources of this uncertainty. As the first step we perform sensitivity analysis on a full N_2/O_2 plasma kinetics model to find a minimal set of processes that are influential for the $R(E/N)$ dependence. It is found to be in agreement with simplified kinetic models generally used. Subsequently, we utilize Monte Carlo-based uncertainty quantification to provide a confidence band for the electric field obtained from the theoretical $R(E/N)$ dependence. Finally, subsequent steps are proposed to significantly reduce the uncertainty of the method.

Keywords: electric field, air kinetics, sensitivity analysis, uncertainty quantification, optical emission spectroscopy, cross-sections, nitrogen spectral bands

1. Introduction

The electric field is an important plasma parameter which determines the electron energy distribution function (EEDF) and, consequently, the plasma kinetics. It governs the production of charged or metastable species and, thereby, the fundamental properties of the plasma itself. The information about the electric field is, therefore, very valuable also for plasmas in air. The possibility to measure the electric field is very instrumental in optimization of air plasma applications

and can facilitate better understanding of atmospheric electricity in a wide range of altitudes/pressures.

The emission spectrum of non-equilibrium low-temperature air discharge extends from UV to near-infrared wavelengths, and is typically composed of many molecular band systems and atomic multiplets [1]. The most dominant are, usually, the first and the second positive systems of molecular nitrogen with the transitions $B^3\Pi_g \rightarrow A^3\Sigma_u^+$ and $C^3\Pi_u \rightarrow B^3\Pi_g$ and the excitation thresholds of radiative states at 7.4 and 11.0 eV, respectively. The emission intensity depends on the population of the excited states produced by the electron-impact processes and the electron energy is given by the local

³ Authors to whom any correspondence should be addressed.

electric field. The above mentioned spectral systems, therefore, carry information about the lower-energy part of the EEDF. In order to get a sensitive spectroscopic signature for the electric field over a wide range of electric fields, the EEDF needs to be probed for higher electron energies as well. Electrons with the energy higher than 18.8 eV produce the emission of the first negative system (FNS) $B^2\Sigma_u^+ \rightarrow X^2\Sigma_g^+$ of N_2^+ . Due to a relatively high threshold for the direct electron-impact ionization from the ground electronic state-of N_2 , the intensity of this system is usually weak, yet detectable, in typical air plasmas, see e.g. in [2].

For the reasons above, the intensity ratio of spectral bands of the FNS and the second positive system (SPS) of N_2 can be used as an indirect non-invasive spectroscopic method of obtaining the reduced electric field in nitrogen containing discharges [3–9]. The ratio itself is typically calculated from the intensity of the FNS (0, 0) band and SPS (0, 0) band. As a consequence of the very different ionization/excitation thresholds mentioned above, the FNS(0, 0)/SPS(0, 0) intensity ratio, denoted $R(E/N)$, is very sensitive to the reduced electric field E/N , with E being magnitude of the electric field, and N the gas number density.

The method has been utilized for measuring the electric field and mean electron energy in corona discharges in ambient air by Gallimberti *et al* already in early 1970s [10]. Then in [3] for measuring the electric field in an atmospheric pressure dielectric barrier discharge in air with sub-nanosecond resolution and resolved in 2D in [11]. Further progress in the application of the method was done in [2], where the time-correlated single photon counting technique was applied to clarify the FNS and SPS emission of streamer both experimentally and theoretically. In [2], a more detailed description of the method's history is given as well. The work [12] used the FNS/SPS ratio method for investigation of negative corona Trichel pulses in heated atmospheric pressure air and for the measured electric field, the authors determined the EEDF and its relaxation. Limitations and fundamental features of the method were also analyzed in [6, 7]. Concerning the discharge phenomena in Earth's atmosphere, the method was applied for transient luminous events such as sprites or blue jets at low pressures (below 10^3 Pa) [4, 13–15]. Several theoretical works also focused on the influence of space and time [16–18] averaging of the optical emissions.

Most recently, the FNS/SPS ratio method has been used for determining the altitude of sprite streamers [19].

The FNS/SPS ratio method relies on the dependence $R(E/N)$ which is, however, pressure, temperature and gas-composition dependent. This means that different conditions have to be taken into account for low pressure and high pressure discharges, and for discharges occurring at low (such as sprites) and elevated (e.g. high repetition rate atmospheric discharges) temperatures. The main reason behind is that radiative losses compete with collisional pressure-dependent quenching at high pressures.

There are two ways of obtaining the $R(E/N)$ dependence, either using a theoretical model with appropriate kinetic data or by means of spectroscopic measurements in a known electric field. Precise experimental determination of $R(E/N)$

faces numerous challenges. It has been performed by Paris *et al* [5] using non-self-sustaining DC discharge in a parallel-plane gap configuration. The discharge was used for determining $R(E/N)$ dependence in air in the pressure range from 300 to 10^5 Pa. It has also been revealed, that for air discharges at pressures above 10 kPa, the ratio $R(E/N)$ is independent of pressure and is solely a function of E/N [5]. The $R(E/N)$ dependence can also be obtained by using a theoretical model but one has to be aware of the uncertainties in the kinetic data, i.e., reaction rate constants and cross-sections. Several models have been constructed with the purpose of the theoretical determination of the $R(E/N)$, e.g. [20–23], each of them providing a somewhat different $R(E/N)$, depending on the kinetic data that have been used. In many cases, however, the choice of the kinetic data and the uncertainty of the model are not discussed.

The aim of this work is to approach the problem of theoretical $R(E/N)$ determination constructing a well-justified model and providing the $R(E/N)$ with its confidence band. To achieve that, we begin with a ‘full kinetic model’ of N_2/O_2 plasma comprising of 617 reactions and perform sensitivity analysis on it using the elementary effects method (EEM) [24] to identify the minimal set of reactions important for the FNS/SPS ratio. On this ‘reduced model’, we perform Monte Carlo-based uncertainty quantification in order to provide a confidence band for theoretical $R(E/N)$ dependence and we identify main sources of uncertainties.

2. FNS/SPS intensity ratio in air

Emission bands typically used for the FNS/SPS intensity ratio determination are the (0, 0) vibronic transitions with band heads located at 337.1 nm for the SPS and at 391.5 nm for the FNS. Based on the simple kinetic model of [3, 12] the generalized formula of the emission intensity ratio is

$$\frac{\frac{dI_{\text{FNS}}}{dt} + \frac{I_{\text{FNS}}}{\tau_{\text{eff}}^{\text{FNS}}} \tau_{\text{eff}}^{\text{FNS}}}{\frac{dI_{\text{SPS}}}{dt} + \frac{I_{\text{SPS}}}{\tau_{\text{eff}}^{\text{SPS}}} \tau_{\text{eff}}^{\text{SPS}}} = R(E/N), \quad (1)$$

where $I_{\text{FNS}, \text{SPS}}$ are the measured intensities of the respective spectral bands and $\tau_{\text{eff}}^{\text{FNS}, \text{SPS}}$ their effective lifetimes. This form is necessary if steady state conditions for emission are not fulfilled, for example in the case of atmospheric pressure air streamers. Note that the omission of time derivative terms in non steady state conditions may lead to significant error in determined electric field [18].

The ratio $R(E/N)$ is however usually calibrated experimentally in a Townsend discharge. In that case the steady state is well-justified and the formula (1) reduces simply to

$$\frac{I_{\text{FNS}}}{I_{\text{SPS}}} = R(E/N). \quad (2)$$

In this work we focus on theoretical determination of $R(E/N)$ for a Townsend-like discharge, where the steady-state conditions are fulfilled.

Table 1. Species considered in the full kinetic model: 12 positive species, 9 negative species, 21 neutral species.

Positive species	N^+ , N_2^+ , N_3^+ , N_4^+ , O^+ , O_2^+ , O_4^+ , NO^+ , N_2O^+ , NO_2^+ , O_2^+ , N_2 , $\text{N}_2^+(\text{B}^2)$
Negative species	e , O^- , O_2^- , O_3^- , O_4^- , NO^- , N_2O^- , NO_2^- , NO_3^-
Neutral species	N_2 , $\text{N}_2(\text{A}^3)$, $\text{N}_2(\text{B}^3)$, $\text{N}_2(\text{a}'^1)$, $\text{N}_2(\text{C}^3)$, N , $\text{N}(\text{D}^2)$, $\text{N}(\text{P}^2)$, O_2 , $\text{O}_2(\text{a}^1)$, $\text{O}_2(\text{b}^1)$, $\text{O}_2(4.5 \text{ eV})$, O , $\text{O}(\text{D}^1)$, $\text{O}(\text{S}^1)$, O_3 , NO , N_2O , NO_2 , NO_3 , N_2O_5

2.1. Kinetic model for FNS/SPS intensity ratio in air

A zero-dimensional chemical kinetic model for dry air ($\text{N}_2\text{--O}_2$, 4:1) at pressure of 10^5 Pa and temperature 300 K , is used to determine the population ratio of $\text{N}_2^+(\text{B}^2\Sigma_u^+)_v=0$ and $\text{N}_2(\text{C}^3\Pi_u)_v=0$ vibrational levels of electronically excited states. To shorten the notation, we further refer to those states simply as $\text{N}_2^+(\text{B}^2)$ and $\text{N}_2(\text{C}^3)$. We base our chemical kinetic model on a list of plasmachemical processes from [25–28] compiled in ZDPlasKin [29] library, input file for $\text{N}_2\text{--O}_2$ mixture (version 1.03). Note that some simplifications have been introduced in the scheme. For example, we discarded vibrational manifolds of N_2 and O_2 ground states. On the other hand, the ZDPlasKin input file does not include processes for $\text{N}_2^+(\text{B}^2)$ and these processes were, therefore, added to the kinetic scheme. The resulting kinetic model used in this work includes a set of 617 chemical reactions listed in the appendix involving 42 species listed in table 1. In order to compare with other experimental and theoretical works dealing with steady state conditions, we seek for a steady state value of the ratio of $\text{N}_2^+(\text{B}^2)$ and $\text{N}_2(\text{C}^3)$ densities. The initial value problem for the resulting ordinary differential equations is integrated in time with the reduced electric field E/N and electron density n_e as fixed parameters. We use an implicit solver radau5 to integrate the stiff reaction system [30]. The complete list of reactions is listed in the table A1. The dependence of the rate constants for electron-impact processes on the reduced electric field E/N is found by solving the Boltzmann equation in the two-term approximation with the use of the BOLSIG+ solver [31] with cross-section sets [32–38]. With 42 species, the kinetic model is fully described by a set of 42 ordinary differential equations. Within this framework the densities of $\text{N}_2(\text{C}^3)$ and $\text{N}_2^+(\text{B}^2)$ obey the following two:

$$\begin{aligned} \frac{d[\text{N}_2(\text{C}^3)]}{dt} &= [e](k_{010}[\text{N}_2] + k_{041}[\text{N}_4^+] \\ &\quad - k_{105}[\text{N}_2(\text{C}^3)] \\ &\quad + k_{124}[\text{N}_2(\text{A}^3)][\text{N}_2(\text{A}^3)] \\ &\quad - [\text{N}_2(\text{C}^3)](k_{129}[\text{N}_2] + k_{130}[\text{O}_2]), \end{aligned} \quad (3)$$

$$\begin{aligned} \frac{d[\text{N}_2^+(\text{B}^2)]}{dt} &= [e]([\text{N}_2]k_{028} + [\text{N}_2^+]k_{050}) \\ &\quad - [\text{N}_2^+(\text{B}^2)]k_{106} \\ &\quad - [\text{N}_2^+(\text{B}^2)][\text{N}_2]([\text{N}_2]k_{366} + [\text{N}]k_{367}) \\ &\quad - [\text{N}_2^+(\text{B}^2)] \left(\sum_{n \in \mathcal{S}} k_n[\text{Y}] - \sum_{m \in \mathcal{T}} k_m[\text{Z}][\text{M}] \right), \end{aligned} \quad (4)$$

where $[\cdot]$ denotes species number density, k_x the rate coefficient for process Px as listed in table A1, and the summations goes

over the set of second order processes $\mathcal{S} := a \{324\text{--}332, 410, 418, 426, 434, 442, 450, 458, 466, 474, 484, 494, 504, 514, 524, 534, 544, 556\}$, and the set of third order processes $\mathcal{T} := a \{562, 568, 574, 585, 593, 601, 609, 617\}$.

The relation between the band emission intensity and the density of the upper excited state $n_{v'}^*$ is given as

$$I_{v'v''} = L \frac{hc}{\lambda_{v'v''}} n_{v'}^* A_{v'v''}, \quad (5)$$

where $v'v''$ defines the vibronic transition, $A_{v'v''}$ is the rate of spontaneous emission (band Einstein coefficient) (s^{-1}) and $\lambda_{v'v''}$ is the characteristic wavelength of emitted radiation during transition between upper (v') and lower (v'') vibronic states. The constant L corresponds to the thickness of the emitting medium, as long as the medium is uniform. This intensity is integrated spectrally over the band as well as over the solid angle and it has the unit of (W m^{-2}).

Finally, the FNS/SPS ratio can be expressed as

$$R(E/N) = \frac{I_{\text{FNS}}}{I_{\text{SPS}}} = \frac{\lambda_{\text{SPS}}[\text{N}_2^+(\text{B}^2)]A_{\text{FNS}}}{\lambda_{\text{FNS}}[\text{N}_2(\text{C}^3)]A_{\text{SPS}}}. \quad (6)$$

Since the densities depend on the reduced electric field through the electron-impact processes, the formula (6) gives the relation between steady state FNS/SPS intensity ratio and the reduced electric field.

3. Methods

3.1. Sensitivity analysis by the EEM

The EEM according to Morris [24] belongs to the family of screening methods. As such, it is capable of identifying inputs, to which a numerical model is insensitive. The main advantage of the method is the number of necessary model evaluations, which is substantially lower compared to variance-based sensitivity analysis methods, e.g. the Sobol method [39]. In contrast to partial-derivative based sensitivity analysis methods [40, 41] used e.g. in [42, 43], EEM scales better with a large number of model inputs. At the same time, the method is capable of detecting nonlinear interactions between the model inputs (e.g. i th input is influential only if j th input is sufficiently large). As the trade-off for the low number of evaluations, the EEM provides only approximate ranking of the importance of the individual model inputs. This is, however, sufficient for reduction of a kinetic scheme, as previously illustrated in [44]. Since the EEM requires that the model inputs be distributed on a unit k -dimensional hypercube, with k being the number of model inputs, we define a

vector of factors $\mathbf{x} = (x_1, \dots, x_k)$, with each x_j is restricted to a finite number of possible choices on $x_j \in [0, 1]$.

The key quantity for the EEM is then the so-called elementary effect. For i th model input, the elementary effect for model output $Y(\mathbf{x})$ is obtained as

$$d_i(\mathbf{x}) = \frac{Y(x_1, \dots, x_i + \Delta, \dots, x_k) - Y(x_1, \dots, x_k)}{\Delta}, \quad (7)$$

where Δ is a constant value by which i th input factor is modified. The Morris' EEM method is based on generating so-called *trajectories* through the configuration space. Each step of Morris trajectory corresponds to a single elementary effect evaluation, proceeding randomly through elements of \mathbf{x} , though, there is exactly one evaluation for each factor per trajectory. To generate trajectories we used basic sampling scheme by Morris [24]. In this way $n = 10^1\text{--}10^2$ elementary effects is required to be generated for each model input to provide sufficient statistics, this corresponds to n trajectories through the hypercube, resulting to a set of n elementary effects $\mathbf{d}_i = \{d_i^1, \dots, d_i^n\}$, for each input i . In this work, we used $n = 100$. Some further improvements for sampling strategy and method efficiency have been proposed in later works, see [45].

Within our work, we apply the EEM to the ‘full kinetic model’ of nitrogen–oxygen plasma in 0D, as described in section 2.1, looking for the FNS/SPS intensity ratio $R(E/N)$ as the output of the model, i.e. the $R(E/N)$ is the observable for the EEM. We aim to determine the sensitivity of $R(E/N)$ to all, k , rate constants which are included in the full kinetic model. The vector $\mathbf{k} = \left(k_1\left(\frac{E}{N}\right), \dots, k_k\left(\frac{E}{N}\right)\right)$ denotes the vector of reaction rates, which have to be varied in order to assess the model sensitivity to these reactions. To link \mathbf{k} with vector of factors \mathbf{x} in the EEM we create a mapping so that

$$k_i\left(\frac{E}{N}\right) = \left(x_i + \frac{1}{2}\right) \cdot k_{0,i}\left(\frac{E}{N}\right), \quad (8)$$

where $k_{0,i}\left(\frac{E}{N}\right)$ is the unperturbed rate coefficient for i th process used in the full kinetic model. This mapping ensures the rate coefficients are varied from $0.5k_{0,i}$ to $1.5k_{0,i}$ and that the model can be expressed consistently with the EEM.

In order to encode output of the model into a single number to be used in (7), we construct L1-error of the time-evolution of the FNS/SPS intensity ratio comparing solutions F and with perturbed and unperturbed rate constants respectively:

$$Y(\mathbf{k}) = \int_0^T |F(\mathbf{k}, t) - F(\mathbf{k}_0, t)| dt, \quad (9)$$

where \mathbf{k} is given by (8) and \mathbf{k}_0 is the unperturbed rate coefficient used in the full kinetic model.

The quantities which reveal whether the model is sensitive to i th input are then the mean value μ_i over the set of n elementary effects \mathbf{d}_i :

$$\mu_i = \frac{1}{n} \sum_{j=1}^n d_i^j, \quad (10)$$

and the standard deviation of the mean, denoted σ_i :

$$\sigma_i = \sqrt{\frac{1}{n} \sum_{j=1}^n (d_i^j - \mu_i)^2}. \quad (11)$$

To be able to conclude that the model is insensitive to i th input, both σ_i and μ_i have to be sufficiently low. A high value of μ_i shows strong linear interaction of the model with the input while a high value of σ_i suggests that there is a non-linear interaction between the output and the input. The choice for the criterion for μ_i and σ_i which distinguishes between influential and non-influential reactions is model-specific and is discussed, for the presented case, in section 4.1.

3.2. Uncertainty quantification

The origin of the uncertainty in calculated $R(E/N)$ is the spread of values in kinetic data, i.e. quenching rates, reaction rates, cross-sections, available in literature. These data were obtained experimentally and the spread is a consequence of both aleatoric (statistical) uncertainties, i.e. the accuracy and noise level of the instrument, and epistemic (systematic) uncertainties, e.g. non-selectivity of the method, different assumptions in data processing. The aleatoric uncertainties can be, in part, eliminated by sufficient statistics, although subtle differences in experimental setups always lead to different values when an experiment is reproduced by different author. The epistemic uncertainties are a much bigger challenge, since their elimination requires deep insight into the methods that have been used for the determination of the kinetic data and assessment of their reliability.

Within this work, we use Monte Carlo-based uncertainty quantification in order to determine the confidence band for the $R(E/N)$. Specifically, we perform 5000 runs of the tested model for each E/N . In each of these runs, the kinetic data for influential processes are randomly varied with uniform distribution within a certain range. The width of the confidence band of the FNS/SPS ratio is then obtained as the maximum and minimum value of the FNS/SPS ratio from the 5000 runs. The range, in which the kinetic data are varied is derived from literature.

4. Results

4.1. Sensitivity analysis and identification of influential processes

In this paragraph we find a reduced kinetic model which, for given electron density n_e and reduced electric field E/N , predicts the same $R(E/N)$ ratio (within the chosen tolerance) as the full kinetic model. The reduction of the kinetic scheme is crucial for the subsequent uncertainty quantification and detailed revision of the kinetic data. In order to identify processes that are influential for $R(E/N)$, we perform sensitivity analysis using EEM on the full kinetic model of 617 reactions. Reduced electric field E/N is varied in the range

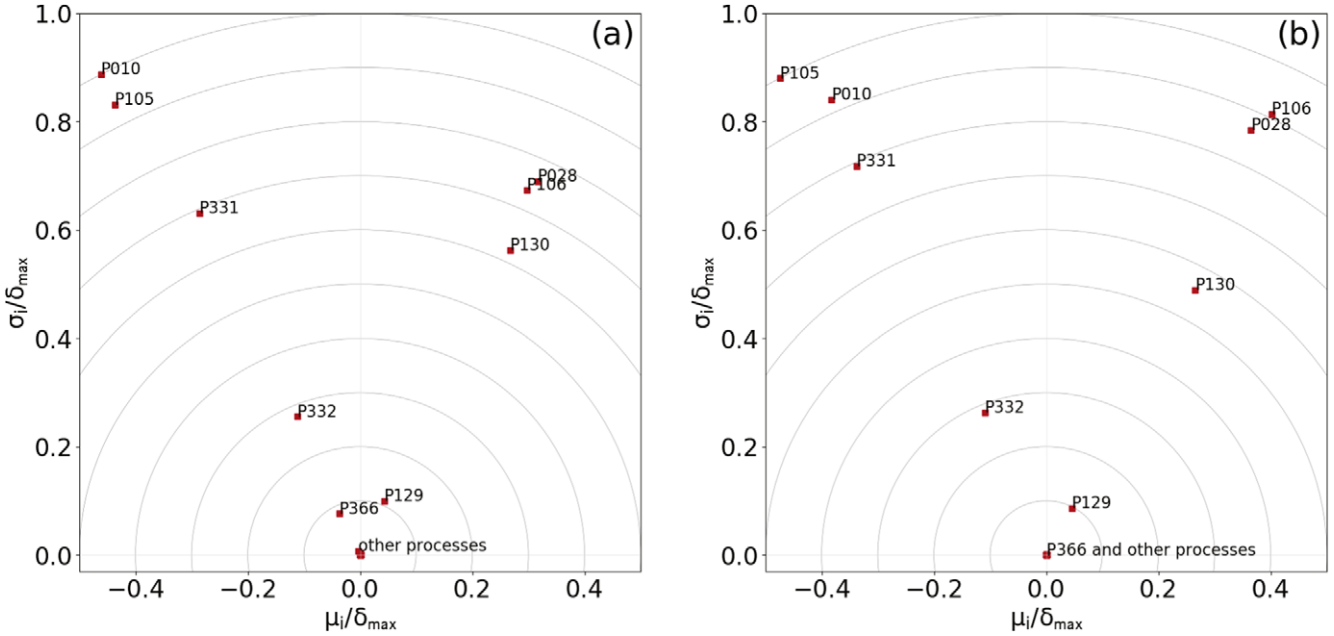


Figure 1. The $\sigma_i-\mu_i$ plot for the EEM analysis. The most important processes for the FNS/SPS ratio are farthest from the origin of the plot. Presented results are for (a) $E/N = 2000$ Td, $n_e = 10^{10}$ cm $^{-3}$; and (b) $E/N = 200$ Td, $n_e = 10^{12}$ cm $^{-3}$. Processes that are considered unimportant are labeled as other processes.

from 100 to 3000 Td. The range for n_e was chosen to represent conditions similar to experimental works [5, 46]. These experiments were performed in a Townsend-like discharge, where the electric field distortion E_s by space charge was checked to be below 1% of the external electric field magnitude E . Considering the experimental setup in [5, 46], we can estimate the maximum value of n_e , for which the discharge still operates in the Townsend mode, by considering an infinite planar plasma slab with thickness of $d = 0.2$ mm filled with uniformly distributed charge of density $q_0 n_e$. For the electric field distortion $E_s/E = 0.01$, the reduced electric field $E/N = 200$ Td, and air number density $N = 2.5 \times 10^{19}$ cm $^{-3}$, the estimated threshold electron density is approximately:

$$n_e = \frac{2\varepsilon_0 E_s E}{dq_0 N} \approx 2.8 \times 10^{10} \text{ cm}^{-3}$$

To cover safely the experimental conditions, we therefore choose n_e to vary from 10^8 to 10^{12} cm $^{-3}$. Further decrease of n_e would not affect the results in terms of the number of influential processes. For the analysis in this section, we use cross-sections from [32, 33] to calculate electron-impact reaction rates. Note that choice of cross-section set is not crucial here, because resulting reaction rates are anyway artificially perturbed on the random walk through the Morris trajectories.

Figure 1 shows the mean value μ_i and standard deviation σ_i of the elementary effects for the most important processes at reduced electric field 2000 Td and electron density $n_e = 10^{10}$ cm $^{-3}$, and at reduced electric field 200 Td and electron density $n_e = 10^{12}$ cm $^{-3}$. Note that μ_i and σ_i where normalized by $\delta_{\max} = \max(\delta_i)$, where $\delta_i = \sqrt{\mu_i^2 + \sigma_i^2}$ is the distance of each point from zero in $\sigma_i-\mu_i$ plot. Processes with values of both μ_i and σ_i close to zero can be considered non-influential for the

model and vice versa. This provides relative ranking for each process considered in the full kinetic model.

Figure 2 shows the relative importance of the 12 most influential processes in terms of δ_i/δ_{\max} , as a function of E/N for $n_e = 10^{10}$ cm $^{-3}$ and $n_e = 10^{12}$ cm $^{-3}$. The choice of the minimum value of δ_i/δ_{\max} for which the processes are still considered influential, is strongly model-specific, and requires heuristic analysis. We have found that using the criterion $\delta_i/\delta_{\max} \geq 0.1$, the maximum relative difference between values of $R(E/N)$ obtained from the full model and the reduced model will be no more than 10^{-2} . The 12 most influential processes are listed in table 2 in the order of importance. There are, in total, 9 processes that meet the $\delta_i/\delta_{\max} \geq 0.1$ criterion. Note that this set of processes includes the three-body quenching of N₂⁺(B²), i.e. the process P366, which was a point of discussion in [23, 47]. It is clear from figure 2 that this process is only important at low values of E/N . Furthermore, in figure 2, we see that electron-impact processes P050 and P023 are getting more influential as the electron density increases and might need to be considered a part of the reduced kinetic model when calculating the FNS/SPS intensity ratio at electron densities higher than 10 12 cm $^{-3}$.

To conclude this section, using the EEM of sensitivity analysis, we were able to reduce the full model of 617 reactions to a minimum model of only 9 reactions, maintaining less than 1% deviation for $R(E/N)$ compared to the full model. Note that this minimal model proofs the model generally used, for instance in [3, 48]. This work mathematically shows that the generally used minimal model does not lack any of the known reactions. And that the three-body quenching which has been disputed in the community

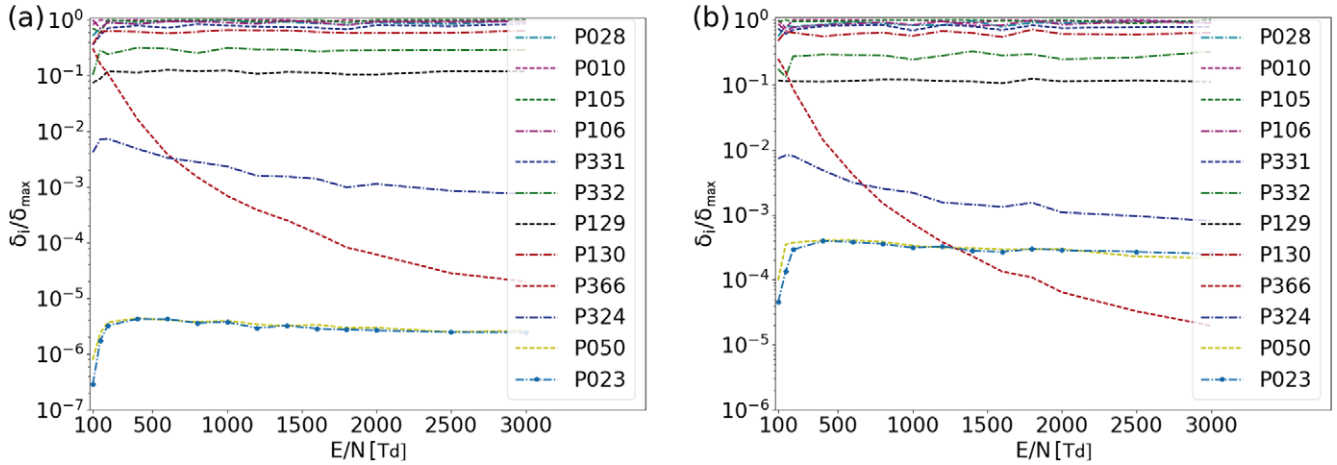


Figure 2. Relative importance of processes in terms of δ_i/δ_{\max} as a function of reduced electric field for fixed densities: (a) $n_e = 10^{10} \text{ cm}^{-3}$, and (b) $n_e = 10^{12} \text{ cm}^{-3}$.

Table 2. The most important processes for the FNS/SPS intensity ratio listed in order of importance. The R1–R9 set defines the *reduced model*. Processes P023 and P050 may be influential for electron densities higher than 10^{12} cm^{-3} . Full spectroscopic notation of species is used in this table: $N_2(X^1\Sigma_g^+)_v=0$, $N_2^+(X^2\Sigma_g^+)_v=0$, $N_2^+(B^2\Sigma_u^+)_v=0$ and $N_2(C^3\Pi_u)_v=0$ is represented by short notation N_2 , N_2^+ , $N_2^+(B^2)$ and $N_2(C^3)$, respectively in table A1.

Reaction no.	Process no.	Reaction
R1	P028	$e + N_2(X^1\Sigma_g^+)_v=0 \longrightarrow N_2^+(B^2\Sigma_u^+)_v'=0 + 2e$
R2	P010	$e + N_2(X^1\Sigma_g^+)_v=0 \longrightarrow N_2(C^3\Pi_u)_v'=0 + e$
R3	P106	$N_2^+(B^2\Sigma_u^+)_v=0 \longrightarrow N_2^+(X^2\Sigma_g^+)_v''=0 + h\nu$
R4	P105	$N_2(C^3\Pi_u)_v'=0 \longrightarrow N_2(B^3\Pi_g)_v''=0 + h\nu$
R5	P331	$N_2^+(B^2\Sigma_u^+)_v=0 + N_2(X^1\Sigma_g^+)_v=0 \longrightarrow N_2^+(X^2\Sigma_g^+)_v=0 + N_2(X^1\Sigma_g^+)_v=0$
R6	P332	$N_2^+(B^2\Sigma_u^+)_v=0 + O_2 \longrightarrow N_2^+(X^2\Sigma_g^+)_v=0 + O + O(^1S)$
R7	P129	$N_2(C^3\Pi_u)_v'=0 + N_2(X^1\Sigma_g^+)_v=0 \longrightarrow N_2(a'1) + N_2(X^1\Sigma_g^+)_v=0$
R8	P130	$N_2(C^3\Pi_u)_v'=0 + O_2 \longrightarrow N_2(X^1\Sigma_g^+)_v=0 + O + O(^1S)$
R9	P366	$N_2^+(B^2\Sigma_u^+)_v'=0 + N_2(X^1\Sigma_g^+)_v=0 + M \longrightarrow N_4^+ + M$
	P324	$N_2^+(B^2\Sigma_u^+)_v=0 + O_2 \longrightarrow O_2^+ + N_2$
	P023	$e + N_2(X^1\Sigma_g^+)_v=0 \longrightarrow N_2^+(X^2\Sigma_g^+)_v''=0 + 2e$
	P050	$e + N_2^+(X^2\Sigma_g^+)_v''=0 \longrightarrow e + N_2^+(B^2\Sigma_u^+)_v=0$

[23, 47] might be of importance, but only at a very low value of the reduced electric field.

For the sake of brevity, the table 2 introduces simplified numbering of the reactions in the reduced model: R1–R9. This numbering is used further on in this work, where we focus on identification and quantification of uncertainties for these reactions.

4.2. Uncertainties in the kinetic data

Using the sensitivity analysis, we obtained a reduced model comprising of only 9 processes. Since there are numerous kinetic data available in literature for these processes, the uncertainty of model should be quantified. To get a deeper insight, we divide the sources of uncertainty into the following four components.

- (i) uncertainty in EEDF,
- (ii) uncertainty in electron-impact cross-sections (R1, R2),

- (iii) uncertainty in radiative de-excitations (R3, R4),
- (iv) uncertainty in quenching rate constants (R5–R9).

The full-range model represents the most straightforward approach to the uncertainty quantification wherein all the kinetic data available in literature are considered in the uncertainty quantification (apart from obvious outliers). The references that have been used for the kinetic data are listed in table 3. The table 3 also includes the exact intervals, in which the individual kinetic parameters were varied.

In the sections below, we briefly discuss the impact of each of the class of processes on the uncertainty in the FNS/SPS ratio. In part II to this publication, we further provide a thorough analysis of these references, deeming some of the values less reliable than others, thereby reducing the model uncertainty.

4.2.1. Uncertainty in EEDF. Both the full and the reduced models utilize BOLSIG+ [133] for calculating the EEDF.

Table 3. Rate constants of the most important processes and relevant interval of experimentally measured data. While there is a good agreement between different references for the quenching rate constants of ($C^3\Pi_u$) state (processes R7 and R8). There are much larger discrepancies in quenching rates that are available in literature for ($B^2\Sigma_u^+$) state (R5 and R6).

No.	Rate constant	Range of kinetic data	References for UQ
R1	$k_{im}^B = \sqrt{\frac{2q_e}{m_e}} \int_0^\infty \epsilon f(\epsilon) \sigma(\epsilon) d\epsilon$	EEDF \times CSS	[49–56]
R2	$k_{im}^C = \sqrt{\frac{2q_e}{m_e}} \int_0^\infty \epsilon f(\epsilon) \sigma(\epsilon) d\epsilon$	EEDF \times CSS	[1, 55, 57–66]
R3	A_{0B}	$(1.11 \div 2.43) \times 10^7 \text{ s}^{-1}$	[67–93]
R4	A_{0C}	$(1.78 \div 3.57) \times 10^7 \text{ s}^{-1}$	[67, 70, 72–75, 78, 82, 86, 89, 91, 92, 94–108]
R5	k_{q,N_2}^B	$(1.37 \div 9.80) \times 10^{-10} \text{ cm}^3 \text{ s}^{-1}$	[75, 78, 82, 84, 85, 91–93, 109–118]
R6	k_{q,O_2}^B	$(4.6 \div 11.0) \times 10^{-10} \text{ cm}^3 \text{ s}^{-1}$	[91, 93, 109, 112, 113, 115, 117, 118]
R7	k_{q,N_2}^C	$(0.40 \div 1.70) \times 10^{-11} \text{ cm}^3 \text{ s}^{-1}$	[82, 91, 94, 96, 98, 100, 108–110, 112, 117–124]
R8	k_{q,O_2}^C	$(1.90 \div 3.30) \times 10^{-10} \text{ cm}^3 \text{ s}^{-1}$	[91, 98, 109, 112, 117–120, 124]
R9	$k_{q,3b}^B = k_0 \left(\frac{T_{\text{gas}}}{T_{\text{eff}}} \right)^{1.6}$	$k_0 \in (5.0 \div 8.5) \times 10^{-29} \text{ cm}^6 \text{ s}^{-1}$	[125–132]

The input settings of BOLSIG+ were ionization degree 10^{-4} , plasma density 10^{12} cm^{-3} and temporal model for growth. Four BOLSIG+ compliant cross-sectional databases are available: Triniti [36], IST Lisbon [37, 38], Biagi [32, 33] and Phelps [34, 35]. Since the cross-sections available in each of these databases differ slightly, the calculated rates of R1 and R2 are influenced and the FNS/SPS ratio will also vary.

If we fix the processes R3–R9 from table 3 on the mean value from interval of their rate coefficients and for processes R1, R2 we use rate coefficients combining electron-impact cross-sections of [56, 64] with different EEDFs obtained from the cross-section libraries (Biagi, Phelps, Triniti, IST Lisbon), we can read the uncertainty of the model from the blue band in figure 3. Specifically, the model gives the electric field ratio anywhere in the range of 440 and 500 Td for the FNS/SPS ratio of 10^{-2} . Compared to the other sources of uncertainty, the cross-sectional databases present only a minor source.

4.2.2. Uncertainty in electron-impact cross-sections of R1 and R2. Subsequently, we varied the electron-impact cross-sections of the processes R1 and R2 within the full-range of data available in literature. From the red band in figure 3, it is apparent that this increases the uncertainty in the electric field distinctly. For the FNS/SPS ratio of 10^{-2} the electric field now lies anywhere in the range between 350 and 560 Td.

4.2.3. Uncertainty in radiative de-excitation lifetimes. When we start varying also the radiative de-excitation lifetimes R3–R4 within the range available in literature (in addition to the electron-impact data discussed above), the uncertainty of the model is further increased. For the FNS/SPS ratio of 10^{-2} is the confidence interval of the electric field 290–740 Td.

4.2.4. Uncertainty in quenching rate constants. Finally, when we also start varying the quenching rate constants R4–R9, there is a further dramatic increase in model uncertainty, as illustrated by the yellow band in figure 3. At the FNS/SPS ratio of 10^{-2} , the predicted electric field now lies anywhere in

the interval 230 and 880 Td. This is also the total uncertainty of the FNS/SPS model.

4.3. Comparison with $R(E/N)$ curves in literature

In figure 4, we plot the total uncertainty band of the model together with theoretical $R(E/N)$ curves obtained by other authors and one experimental. It is apparent that all the curves available in literature lie within the confidence band, as they should since the authors constructing these models worked with equivalent literature. This illustrates that the theoretical $R(E/N)$ curve has very large uncertainty that has to be considered in data processing using this method. Considering that the electric field measured by the intensity ratio method might be further utilized for calculating the plasma kinetics and that electron-impact reactions often show exponential dependence on E/N , we can assert that reducing the $R(E/N)$ uncertainty is very desirable.

Summarizing the results above, the differences among considered cross-section datasets present only a minor source of uncertainty of the theoretical $R(E/N)$ curves.

On the other hand, the ionization and excitation cross-sections for the $N_2^+(B^2)$ and $N_2(C^3)$ states, as well as their quenching rates and radiative lifetimes all present substantial sources of uncertainty. Taking all of them into account, we find that the total uncertainty of the $R(E/N)$ curves is very significant. The spread of $R(E/N)$ curves available in literature confirms that there is no agreement in the community as to which kinetic data should be used for obtaining $R(E/N)$.

4.4. Spectrometric considerations

Figure 5 shows the synthetic spectra of SPS and FNS generated using models detailed in [1]. It should be underlined that in the case of FNS most of the emission originating from the $v = 0$ vibrational level goes indeed through the $v' = 0 \rightarrow v'' = 0$ transition, therefore the (0, 0) band of the FNS is the obvious choice for detection. However, in the case of the SPS emission, there are other options because several bands originating from the $v = 0$ level of the $N_2(C^3\Pi_u)$ state occur with sufficient intensities, e.g. (0, 1), (0, 2) or (0, 3)

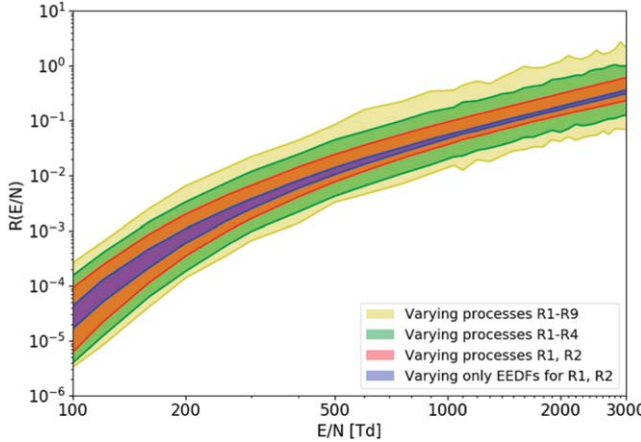


Figure 3. The uncertainty of the FNS/SPS ratio calculated by varying the kinetic data in the reduced model. With each band, a new source of uncertainty is introduced. The largest yellow band is the overall uncertainty of the model, when considering all the kinetic data available in literature.

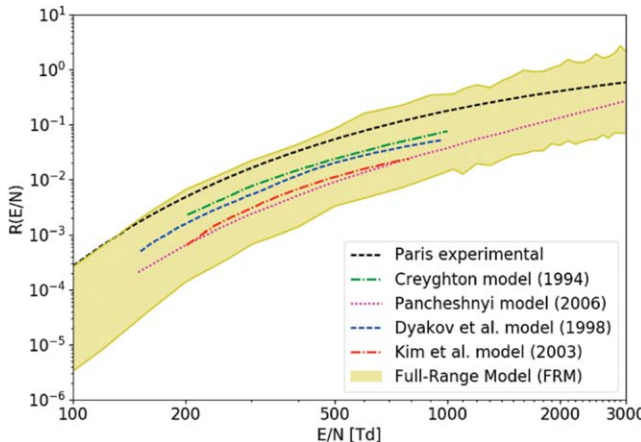


Figure 4. Comparison of the total confidence band of the FNS/SPS model with $R(E/N)$ curves published in earlier works.

bands indicated by arrows in the figure 5 at 357.7, 380.5 and 405.9 nm, respectively. Considering that the detection efficiency often increases from UV to visible spectral range, the combination of FNS(0, 0) and SPS(0, 2), or FNS(0, 0) and SPS(0, 3) might be better choice compared with the FNS(0, 0) and SPS(0, 0) case. This is certainly true in the case of remote spectrometric observation of transient luminous events because of heavy attenuation of the UV part of emission spectra, including the SPS(0, 0) band intensity. It is worth noting that Paris *et al* [5] also quantified the electric field dependence for the ratios of FNS(0, 0)/SPS(2, 5) and SPS(2, 5)/SPS(0, 0). The variation of the SPS(2, 5)/SPS(0, 0) intensity ratio in the low field region <300 Td is consistent with predicted E/N dependence of the rate constant for electron-impact excitation of individual vibration levels of the $C^3\Pi_u$ state [1]. A similar variation with the E/N should be obtained for other SPS bands, the (3, 6) and (1, 4) bands, occurring next or close to the FNS(0, 0) band (see figure 5). The FNS(0, 0)/SPS(3, 6) and FNS(0, 0)/SPS(1, 4) might provide alternative $R(E/N)$ curves to be used simultaneously

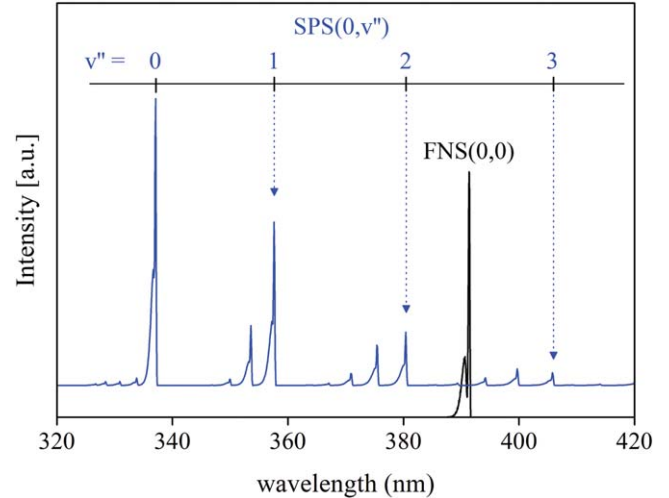


Figure 5. Synthetic emission spectra of the second positive system of N_2 and (0, 0) band of the first negative system of N_2^+ . Calculated using triangular instrumental function and rotational temperature of 300 K. Spectrometric representation of the FCF-like vibrational distribution of the $N_2(C^3\Pi_u)$ state defined by Franck–Condon factors between ($C^3\Pi_u$, $v = 0$ –4) and ($X^1\Sigma_g^+$, $v = 0$) levels.

with $R(E/N)$ curves derived from FNS(0, 0)/SPS(0, 3) and FNS(0, 0)/SPS(2, 5).

Each of these ratios dependences represents a diagnostic tool for the determination of the reduced electric field. Each of these dependencies would require additional uncertainty quantification, which would also consider the uncertainty in the respective vibrational transitions and Frank–Condon factors. However, the 9 influential processes identified in this work are also valid for other FNS/SPS bands.

5. Conclusions

This work focuses on the intensity ratio method for the determination of the electric field in N_2/O_2 plasmas with the aim to evaluate the main sources of uncertainty in the $R(E/N)$ curve and to quantify the total uncertainty of the method. Since the theoretical $R(E/N)$ curve is obtained by solving the non-equilibrium kinetics in N_2/O_2 mixture, we first utilized sensitivity analysis according to Morris [24] to identify the key pathways leading to the population of the radiative N_2 states, from which the FNS/SPS ratio is measured. The sensitivity analysis has revealed that 9 reactions are influential for the population and de-population of the $N_2^+(B^2\Sigma_g^+)$ and $N_2(C^3\Pi_u)$ states. To be able to compare the sensitivity analysis to Townsend discharge-based experimental calibration curve by [5], we carried it out at the values of electron density and reduced electric field that are relevant to the Townsend discharge conditions. It is worth noting that these 9 processes have generally been considered important by the authors developing and improving the intensity ratio method. This work provides a sound mathematical justification for this choice. It also gives insight into the importance of three-body quenching which has been discussed in the community and which we have shown to only gain importance at low electric fields. Consequently, we varied the

rate constants of these 9 most influential processes within the range of values available in literature. We arrived at the conclusion that the total uncertainty of the $R(E/N)$ curve is as large as half an order of magnitude. By quantifying the uncertainty, we provide the community with the confidence interval for the $R(E/N)$ curve. Knowing that the confidence band is very broad and knowing the processes which cause the uncertainty is a necessary starting point for reducing this uncertainty and obtaining a more accurate $R(E/N)$. In part II to this publication, we take the first step in this direction, carefully revising the kinetic data available in literature and constructing a ‘state-of-the-art model’ with substantially reduced uncertainty of the $R(E/N)$ curve. In a more general perspective, this work presents a suitable methodology for approaching plasma kinetics calculations. The goal of a complex plasma model is often to predict a single or a few quantities. By applying a method of sensitivity analysis, we isolate only those processes that are influential for the desired model output. Consequently, we quantify, how the uncertainty of the model inputs manifests in the overall uncertainty of the model predictions. Supplying the model prediction together with its uncertainty should be a best practice when comparing theoretical predictions to experimental results or to each other.

Acknowledgments

This work was supported by the Czech Science Foundation research project 15-04023S and partially support of project LO1411 (NPU I) funded by the Ministry of Education, Youth and Sports of the Czech Republic. ZB acknowledges discussions with Dr Nikolay A Popov concerning three-body quenching. Computational resources were supplied by the Ministry of Education, Youth and Sports of the Czech Republic under the Projects CESNET (Project No. LM2015042) and CERIT-Scientific Cloud (Project No. LM2015085) provided within the program Projects of Large Research, Development and Innovations Infrastructures.

Appendix. Kinetic scheme

This appendix provides the full kinetic scheme as discussed in section 2.1. This kinetic scheme is based on works [25–28] as compiled in ZDPlasKin [29] library, input file for N₂–O₂ mixture (version 1.03). The following effective temperatures

Table A1. Full kinetic scheme for air plasma.

No.	Reaction	Rate coefficient
P001	$e + N_2 \rightarrow e + N_2(A^3, v = 0\text{--}4)$	$f(E/N)$
P002	$e + N_2 \rightarrow e + N_2(A^3, v = 5\text{--}9)$	$f(E/N)$
P003	$e + N_2 \rightarrow e + N_2(A^3, v > 10)$	$f(E/N)$
P004	$e + N_2 \rightarrow e + N_2(B^3)$	$f(E/N)$
P005	$e + N_2 \rightarrow e + N_2(W^3)$	$f(E/N)$
P006	$e + N_2 \rightarrow e + N_2(B'^3)$	$f(E/N)$
P007	$e + N_2 \rightarrow e + N_2(a^1)$	$f(E/N)$
P008	$e + N_2 \rightarrow e + N_2(a^1)$	$f(E/N)$
P009	$e + N_2 \rightarrow e + N_2(w^1)$	$f(E/N)$
P010	$e + N_2 \rightarrow e + N_2(C^3)$	$f(E/N)$
P011	$e + N_2 \rightarrow e + N + N^{(2)D}$	$f(E/N)$
P012	$e + O_2 \rightarrow e + O_2(a^1)$	$f(E/N)$
P013	$e + O_2 \rightarrow e + O_2(b^1)$	$f(E/N)$
P014	$e + O_2 \rightarrow e + O_2(4.5\text{ eV})$	$f(E/N)$
P015	$e + O_2 \rightarrow e + O + O$	$f(E/N)$
P016	$e + O_2 \rightarrow e + O + O(^1D)$	$f(E/N)$
P017	$e + O_2 \rightarrow e + O + O(^1S)$	$f(E/N)$
P018	$e + O_2(a^1) \rightarrow e + O + O$	$f(E/N)$
P019	$e + O \rightarrow e + O(^1D)$	$f(E/N)$
P020	$e + O \rightarrow e + O(^1S)$	$f(E/N)$
P021	$e + N \rightarrow e + e + N^+$	$f(E/N)$
P022	$e + O \rightarrow e + e + O^+$	$f(E/N)$
P023	$e + N_2 \rightarrow e + e + N_2^+$	$f(E/N)$
P024	$e + N_2(A^3) \rightarrow e + e + N_2^+$	$f(E/N)$
P025	$e + O_2 \rightarrow e + e + O_2^+$	$f(E/N)$
P026	$e + O_2(a^1) \rightarrow e + e + O_2^+$	$f(E/N)$
P027	$e + NO \rightarrow e + e + NO^+$	$f(E/N)$
P028	$e + N_2 \rightarrow e + e + N_2^+(B^2)$	$f(E/N)$
P029	$e + NO \rightarrow e + e + N^+ + O$	$f(E/N)$
P030	$e + NO \rightarrow e + e + N + O^+$	$f(E/N)$
P031	$e + N_2O \rightarrow e + e + N_2O^+$	$f(E/N)$
P032	$e + N_2^+ \rightarrow N + N$	$1.8e-7^*(300.0/\text{Te})^{**0.39*0.50}$
P033	$e + N_2^+ \rightarrow N + N(^2D)$	$1.8e-7^*(300.0/\text{Te})^{**0.39*0.45}$

Table A1. (Continued.)

No.	Reaction	Rate coefficient
P034	$e + N_2^+ \rightarrow N + N(^2P)$	$1.8e-7^*(300.0/T_e)^{**0.39}*0.05$
P035	$e + O_2^+ \rightarrow O + O$	$2.7e-7^*(300.0/T_e)^{**0.7}*0.55$
P036	$e + O_2^+ \rightarrow O + O(^1D)$	$2.7e-7^*(300.0/T_e)^{**0.7}*0.40$
P037	$e + O_2^+ \rightarrow O + O(^1S)$	$2.7e-7^*(300.0/T_e)^{**0.7}*0.05$
P038	$e + NO^+ \rightarrow O + N$	$4.2e-7^*(300.0/T_e)^{**0.85}*0.20$
P039	$e + NO^+ \rightarrow O + N(^2D)$	$4.2e-7^*(300.0/T_e)^{**0.85}*0.80$
P040	$e + N_3^+ \rightarrow N_2 + N$	$2.0e-7^*(300.0/T_e)^{**0.5}$
P041	$e + N_4^+ \rightarrow N_2 + N_2(C^3)$	$2.3e-6^*(300.0/T_e)^{**0.53}$
P042	$e + N_2O^+ \rightarrow N_2 + O$	$2.0e-7^*(300.0/T_e)^{**0.5}$
P043	$e + NO_2^+ \rightarrow NO + O$	$2.0e-7^*(300.0/T_e)^{**0.5}$
P044	$e + O_4^+ \rightarrow O_2 + O_2$	$1.4e-6^*(300.0/T_e)^{**0.5}$
P045	$e + O_2^+ N_2 \rightarrow O_2 + N_2$	$1.3e-6^*(300.0/T_e)^{**0.5}$
P046	$e + N^+ + e \rightarrow N + e$	$7.0e-20^*(300.0/T_e)^{**4.5}$
P047	$e + O^+ + e \rightarrow O + e$	$7.0e-20^*(300.0/T_e)^{**4.5}$
P048	$e + N^+ + M \rightarrow N + M$	$6.0e-27^*(300.0/T_e)^{**1.5}$
P049	$e + O^+ + M \rightarrow O + M$	$6.0e-27^*(300.0/T_e)^{**1.5}$
P050	$e + N_2^+ \rightarrow N_2^+(B^2) + e$	$f(E/N)$
P051	$e + O_2 \rightarrow O^- + O$	$f(E/N)$
P052	$e + NO \rightarrow O^- + N$	$f(E/N)$
P053	$e + O_3 \rightarrow O^- + O_2$	$f(E/N)$
P054	$e + O_3 \rightarrow O_2^- + O$	$f(E/N)$
P055	$e + O_2(a^1) \rightarrow O + O^-$	$f(E/N)$
P056	$e + O_2 + O_2 \rightarrow O_2^- + O_2$	$f(E/N)$
P057	$e + NO_2 \rightarrow O^- + NO$	$1.0e-11$
P058	$e + O + O_2 \rightarrow O^- + O_2$	$1.0e-31$
P059	$e + O + O_2 \rightarrow O_2^- + O$	$1.0e-31$
P060	$e + O_3 + M \rightarrow O_3^- + M$	$1.0e-31$
P061	$e + NO + M \rightarrow NO^- + M$	$8.0e-31$
P062	$e + N_2O + M \rightarrow N_2O^- + M$	$6.0e-33$
P063	$e + O_2 + N_2 \rightarrow O_2^- + N_2$	$1.1e-31^*(300.0/T_e)^{**2} * \exp(-70.0/T_{gas}) * \exp(1500.0^*(T_e - T_{gas}) / (T_e * T_{gas}))$
P064	$O^- + O \rightarrow O_2 + e$	$1.4e-10$
P065	$O^- + N \rightarrow NO + e$	$2.6e-10$
P066	$O^- + NO \rightarrow NO_2 + e$	$2.6e-10$
P067	$O^- + N_2 \rightarrow N_2O + e$	$5.0e-13$
P068	$O^- + O_2 \rightarrow O_3 + e$	$5.0e-15$
P069	$O^- + O_2(a^1) \rightarrow O_3 + e$	$3.0e-10$
P070	$O^- + O_2(b^1) \rightarrow O + O_2 + e$	$6.9e-10$
P071	$O^- + N_2(A^3) \rightarrow O + N_2 + e$	$2.2e-9$
P072	$O^- + N_2(B^3) \rightarrow O + N_2 + e$	$1.9e-9$
P073	$O^- + O_3 \rightarrow O_2 + O_2 + e$	$3.0e-10$
P074	$O_2^- + O \rightarrow O_3 + e$	$1.5e-10$
P075	$O_2^- + N \rightarrow NO_2 + e$	$5.0e-10$
P076	$O_2^- + O_2 \rightarrow O_2 + O_2 + e$	$2.7e-10^*(T_{effN2}/300.0)^{**0.5} * \exp(-5590.0/T_{effN2})$
P077	$O_2^- + O_2(a^1) \rightarrow O_2 + O_2 + e$	$2.0e-10$
P078	$O_2^- + O_2(b^1) \rightarrow O_2 + O_2 + e$	$3.6e-10$
P079	$O_2^- + N_2 \rightarrow O_2 + N_2 + e$	$1.9e-12^*(T_{effN2}/300.0)^{**0.5} * \exp(-4990.0/T_{effN2})$
P080	$O_2^- + N_2(A^3) \rightarrow O_2 + N_2 + e$	$2.1e-9$
P081	$O_2^- + N_2(B^3) \rightarrow O_2 + N_2 + e$	$2.5e-9$
P082	$O_3^- + O \rightarrow O_2 + O_2 + e$	$3.0e-10$
P083	$NO^- + N \rightarrow N_2O + e$	$5.0e-10$
P084	$O_3^- + N \rightarrow NO + O_2 + e$	$5.0e-10$
P085	$N_2O^- + N \rightarrow NO + N_2 + e$	$5.0e-10$
P086	$NO_2^- + N \rightarrow NO + NO + e$	$5.0e-10$
P087	$NO_3^- + N \rightarrow NO + NO_2 + e$	$5.0e-10$
P088	$NO^- + O \rightarrow NO_2 + e$	$1.5e-10$
P089	$N_2O^- + O \rightarrow NO + NO + e$	$1.5e-10$
P090	$NO_2^- + O \rightarrow NO + O_2 + e$	$1.5e-10$

Table A1. (Continued.)

No.	Reaction	Rate coefficient
P091	$\text{NO}_3^- + \text{O} \rightarrow \text{NO} + \text{O}_3 + \text{e}$	1.5e-10
P092	$\text{O}_3^- + \text{N}_2(\text{A}^3) \rightarrow \text{O}_3 + \text{N}_2 + \text{e}$	2.1e-9
P093	$\text{NO}^- + \text{N}_2(\text{A}^3) \rightarrow \text{NO} + \text{N}_2 + \text{e}$	2.1e-9
P094	$\text{N}_2\text{O}^- + \text{N}_2(\text{A}^3) \rightarrow \text{N}_2\text{O} + \text{N}_2 + \text{e}$	2.1e-9
P095	$\text{NO}_2 + \text{N}_2(\text{A}^3) \rightarrow \text{NO}_2 + \text{N}_2 + \text{e}$	2.1e-9
P096	$\text{NO}_3^- + \text{N}_2(\text{A}^3) \rightarrow \text{NO}_3 + \text{N}_2 + \text{e}$	2.1e-9
P097	$\text{O}_3^- + \text{N}_2(\text{B}^3) \rightarrow \text{O}_3 + \text{N}_2 + \text{e}$	2.5e-9
P098	$\text{NO}^- + \text{N}_2(\text{B}^3) \rightarrow \text{NO} + \text{N}_2 + \text{e}$	2.5e-9
P099	$\text{N}_2\text{O}^- + \text{N}_2(\text{B}^3) \rightarrow \text{N}_2\text{O} + \text{N}_2 + \text{e}$	2.5e-9
P100	$\text{NO}_2^- + \text{N}_2(\text{B}^3) \rightarrow \text{NO}_2 + \text{N}_2 + \text{e}$	2.5e-9
P101	$\text{NO}_3^- + \text{N}_2(\text{B}^3) \rightarrow \text{NO}_3 + \text{N}_2 + \text{e}$	2.5e-9
P102	$\text{N}_2(\text{A}^3) \rightarrow \text{N}_2$	0.50
P103	$\text{N}_2(\text{B}^3) \rightarrow \text{N}_2(\text{A}^3)$	1.34e5
P104	$\text{N}_2(\text{a}^1) \rightarrow \text{N}_2$	1.0e2
P105	$\text{N}_2(\text{C}^3) \rightarrow \text{N}_2(\text{B}^3)$	2.39e7
P106	$\text{N}_2^+(\text{B}^2) \rightarrow \text{N}_2^+$	1.6e7
P107	$\text{O}_2(\text{a}^1) \rightarrow \text{O}_2$	2.6e-4
P108	$\text{O}_2(\text{b}^1) \rightarrow \text{O}_2(\text{a}^1)$	1.5e-3
P109	$\text{O}_2(\text{b}^1) \rightarrow \text{O}_2$	8.5e-2
P110	$\text{O}_2(4.5\text{eV}) \rightarrow \text{O}_2$	11.0
P111	$\text{N}_2(\text{A}^3) + \text{O} \rightarrow \text{NO} + \text{N}(\text{D})$	7.0e-12
P112	$\text{N}_2(\text{A}^3) + \text{O} \rightarrow \text{N}_2 + \text{O}(\text{S})$	2.1e-11
P113	$\text{N}_2(\text{A}^3) + \text{N} \rightarrow \text{N}_2 + \text{N}$	2.0e-12
P114	$\text{N}_2(\text{A}^3) + \text{N} \rightarrow \text{N}_2 + \text{N}(\text{P})$	4.0e-11 * (300.0 / Tgas) ** 0.667
P115	$\text{N}_2(\text{A}^3) + \text{O}_2 \rightarrow \text{N}_2 + \text{O} + \text{O}(\text{D})$	2.1e-12 * (Tgas / 300.0) ** 0.55
P116	$\text{N}_2(\text{A}^3) + \text{O}_2 \rightarrow \text{N}_2 + \text{O}_2(\text{a}^1)$	2.0e-13 * (Tgas / 300.0) ** 0.55
P117	$\text{N}_2(\text{A}^3) + \text{O}_2 \rightarrow \text{N}_2 + \text{O}_2(\text{b}^1)$	2.0e-13 * (Tgas / 300.0) ** 0.55
P118	$\text{N}_2(\text{A}^3) + \text{O}_2 \rightarrow \text{N}_2\text{O} + \text{O}$	2.0e-14 * (Tgas / 300.0) ** 0.55
P119	$\text{N}_2(\text{A}^3) + \text{N}_2 \rightarrow \text{N}_2 + \text{N}_2$	3.0e-16
P120	$\text{N}_2(\text{A}^3) + \text{NO} \rightarrow \text{N}_2 + \text{NO}$	6.9e-11
P121	$\text{N}_2(\text{A}^3) + \text{N}_2\text{O} \rightarrow \text{N}_2 + \text{N} + \text{NO}$	1.0e-11
P122	$\text{N}_2(\text{A}^3) + \text{NO}_2 \rightarrow \text{N}_2 + \text{O} + \text{NO}$	1.0e-12
P123	$\text{N}_2(\text{A}^3) + \text{N}_2(\text{A}^3) \rightarrow \text{N}_2 + \text{N}_2(\text{B}^3)$	3.0e-10
P124	$\text{N}_2(\text{A}^3) + \text{N}_2(\text{A}^3) \rightarrow \text{N}_2 + \text{N}_2(\text{C}^3)$	1.5e-10
P125	$\text{N}_2(\text{B}^3) + \text{N}_2 \rightarrow \text{N}_2(\text{A}^3) + \text{N}_2$	3.0e-11
P126	$\text{N}_2(\text{B}^3) + \text{N}_2 \rightarrow \text{N}_2 + \text{N}_2$	2.0e-12
P127	$\text{N}_2(\text{B}^3) + \text{O}_2 \rightarrow \text{N}_2 + \text{O} + \text{O}$	3.0e-10
P128	$\text{N}_2(\text{B}^3) + \text{NO} \rightarrow \text{N}_2(\text{A}^3) + \text{NO}$	2.4e-10
P129	$\text{N}_2(\text{C}^3) + \text{N}_2 \rightarrow \text{N}_2(\text{a}^1) + \text{N}_2$	1.32e-11
P130	$\text{N}_2(\text{C}^3) + \text{O}_2 \rightarrow \text{N}_2 + \text{O} + \text{O}(\text{S})$	2.9e-10
P131	$\text{N}_2(\text{a}^1) + \text{N}_2 \rightarrow \text{N}_2(\text{B}^3) + \text{N}_2$	1.9e-13
P132	$\text{N}_2(\text{a}^1) + \text{O}_2 \rightarrow \text{N}_2 + \text{O} + \text{O}$	2.8e-11
P133	$\text{N}_2(\text{a}^1) + \text{NO} \rightarrow \text{N}_2 + \text{N} + \text{O}$	3.6e-10
P134	$\text{N}_2(\text{a}^1) + \text{N}_2(\text{A}^3) \rightarrow \text{N}_4^+ + \text{e}$	4.0e-12
P135	$\text{N}_2(\text{a}^1) + \text{N}_2(\text{a}^1) \rightarrow \text{N}_4^+ + \text{e}$	1.0e-11
P136	$\text{N} + \text{N} + \text{N}_2 \rightarrow \text{N}_2(\text{A}^3) + \text{N}_2$	1.7e-33
P137	$\text{N} + \text{N} + \text{O}_2 \rightarrow \text{N}_2(\text{A}^3) + \text{O}_2$	1.7e-33
P138	$\text{N} + \text{N} + \text{NO} \rightarrow \text{N}_2(\text{A}^3) + \text{NO}$	1.7e-33
P139	$\text{N} + \text{N} + \text{N} \rightarrow \text{N}_2(\text{A}^3) + \text{N}$	1.0e-32
P140	$\text{N} + \text{N} + \text{O} \rightarrow \text{N}_2(\text{A}^3) + \text{O}$	1.0e-32
P141	$\text{N} + \text{N} + \text{N}_2 \rightarrow \text{N}_2(\text{B}^3) + \text{N}_2$	2.4e-33
P142	$\text{N} + \text{N} + \text{O}_2 \rightarrow \text{N}_2(\text{B}^3) + \text{O}_2$	2.4e-33
P143	$\text{N} + \text{N} + \text{NO} \rightarrow \text{N}_2(\text{B}^3) + \text{NO}$	2.4e-33
P144	$\text{N} + \text{N} + \text{N} \rightarrow \text{N}_2(\text{B}^3) + \text{N}$	1.4e-32
P145	$\text{N} + \text{N} + \text{O} \rightarrow \text{N}_2(\text{B}^3) + \text{O}$	1.4e-32
P146	$\text{N}(\text{D}) + \text{O} \rightarrow \text{N} + \text{O}(\text{D})$	4.0e-13
P147	$\text{N}(\text{D}) + \text{O}_2 \rightarrow \text{NO} + \text{O}$	5.2e-12
P148	$\text{N}(\text{D}) + \text{NO} \rightarrow \text{N}_2 + \text{O}$	1.8e-10
P149	$\text{N}(\text{D}) + \text{N}_2\text{O} \rightarrow \text{NO} + \text{N}_2$	3.5e-12

Table A1. (Continued.)

No.	Reaction	Rate coefficient
P150	$N(^2D) + N_2 \rightarrow N + N_2$	$1.0e-13 * \exp(-510.0/T_{gas})$
P151	$N(^2P) + N \rightarrow N + N$	$1.8e-12$
P152	$N(^2P) + O \rightarrow N + O$	$1.0e-12$
P153	$N(^2P) + N \rightarrow N(^2D) + N$	$6.0e-13$
P154	$N(^2P) + N_2 \rightarrow N + N_2$	$6.0e-14$
P155	$N(^2P) + N(^2D) \rightarrow N_2^+ + e^-$	$1.0e-13$
P156	$N(^2P) + O_2 \rightarrow NO + O$	$2.6e-12$
P157	$N(^2P) + NO \rightarrow N_2(A^3) + O$	$3.0e-11$
P158	$O_2(a^1) + O \rightarrow O_2 + O$	$7.0e-16$
P159	$O_2(a^1) + N \rightarrow NO + O$	$2.0e-14 * \exp(-600.0/T_{gas})$
P160	$O_2(a^1) + O_2 \rightarrow O_2 + O_2$	$3.8e-18 * \exp(-205.0/T_{gas})$
P161	$O_2(a^1) + N_2 \rightarrow O_2 + N_2$	$3.0e-21$
P162	$O_2(a^1) + NO \rightarrow O_2 + NO$	$2.5e-11$
P163	$O_2(a^1) + O_3 \rightarrow O_2 + O_2 + O(^1D)$	$5.2e-11 * \exp(-2840.0/T_{gas})$
P164	$O_2(a^1) + O_2(a^1) \rightarrow O_2 + O_2(b^1)$	$7.0e-28 * T_{gas}^{**3.8} * \exp(700.0/T_{gas})$
P165	$O + O_3 \rightarrow O_2 + O_2(a^1)$	$1.0e-11 * \exp(-2300.0/T_{gas})$
P166	$O_2(b^1) + O \rightarrow O_2(a^1) + O$	$8.1e-14$
P167	$O_2(b^1) + O \rightarrow O_2 + O(^1D)$	$3.4e-11 * (300.0/T_{gas})^{**0.1} * \exp(-4200.0/T_{gas})$
P168	$O_2(b^1) + O_2 \rightarrow O_2(a^1) + O_2$	$4.3e-22 * T_{gas}^{**2.4} * \exp(-281.0/T_{gas})$
P169	$O_2(b^1) + N_2 \rightarrow O_2(a^1) + N_2$	$1.7e-15 * (T_{gas}/300.0)$
P170	$O_2(b^1) + NO \rightarrow O_2(a^1) + NO$	$6.0e-14$
P171	$O_2(b^1) + O_3 \rightarrow O_2 + O_2 + O$	$2.2e-11$
P172	$O_2(4.5\text{ eV}) + O \rightarrow O_2 + O(^1S)$	$9.0e-12$
P173	$O_2(4.5\text{ eV}) + O_2 \rightarrow O_2(b^1) + O_2(b^1)$	$3.0e-13$
P174	$O_2(4.5\text{ eV}) + N_2 \rightarrow O_2(b^1) + N_2$	$9.0e-15$
P175	$O(^1D) + O \rightarrow O + O$	$8.0e-12$
P176	$O(^1D) + O_2 \rightarrow O + O_2$	$6.4e-12 * \exp(67.0/T_{gas})$
P177	$O(^1D) + O_2 \rightarrow O + O_2(a^1)$	$1.0e-12$
P178	$O(^1D) + O_2 \rightarrow O + O_2(b^1)$	$2.6e-11 * \exp(67.0/T_{gas})$
P179	$O(^1D) + N_2 \rightarrow O + N_2$	$2.3e-11$
P180	$O(^1D) + O_3 \rightarrow O_2 + O + O$	$1.2e-10$
P181	$O(^1D) + O_3 \rightarrow O_2 + O_2$	$1.2e-10$
P182	$O(^1D) + NO \rightarrow O_2 + N$	$1.7e-10$
P183	$O(^1D) + N_2O \rightarrow NO + NO$	$7.2e-11$
P184	$O(^1D) + N_2O \rightarrow O_2 + N_2$	$4.4e-11$
P185	$O(^1S) + O \rightarrow O(^1D) + O$	$5.0e-11 * \exp(-300.0/T_{gas})$
P186	$O(^1S) + N \rightarrow O + N$	$1.0e-12$
P187	$O(^1S) + O_2 \rightarrow O(^1D) + O_2$	$1.3e-12 * \exp(-850.0/T_{gas})$
P188	$O(^1S) + O_2 \rightarrow O + O + O$	$3.0e-12 * \exp(-850.0/T_{gas})$
P189	$O(^1S) + N_2 \rightarrow O + N_2$	$1.0e-17$
P190	$O(^1S) + O_2(a^1) \rightarrow O + O_2(4.5\text{ eV})$	$1.1e-10$
P191	$O(^1S) + O_2(a^1) \rightarrow O(^1D) + O_2(b^1)$	$2.9e-11$
P192	$O(^1S) + O_2(a^1) \rightarrow O + O + O$	$3.2e-11$
P193	$O(^1S) + NO \rightarrow O + NO$	$2.9e-10$
P194	$O(^1S) + NO \rightarrow O(^1D) + NO$	$5.1e-10$
P195	$O(^1S) + O_3 \rightarrow O_2 + O_2$	$2.9e-10$
P196	$O(^1S) + O_3 \rightarrow O_2 + O + O(^1D)$	$2.9e-10$
P197	$O(^1S) + N_2O \rightarrow O + N_2O$	$6.3e-12$
P198	$O(^1S) + N_2O \rightarrow O(^1D) + N_2O$	$3.1e-12$
P199	$N + NO \rightarrow O + N_2$	$1.8e-11 * (T_{gas}/300.0)^{**0.5}$
P200	$N + O_2 \rightarrow O + NO$	$3.2e-12 * (T_{gas}/300.0)^{*} \exp(-3150.0/T_{gas})$
P201	$N + NO_2 \rightarrow O + O + N_2$	$9.1e-13$
P202	$N + NO_2 \rightarrow O + N_2O$	$3.0e-12$
P203	$N + NO_2 \rightarrow N_2 + O_2$	$7.0e-13$
P204	$N + NO_2 \rightarrow NO + NO$	$2.3e-12$
P205	$O + N_2 \rightarrow N + NO$	$3.0e-10 * \exp(-38370.0/T_{gas})$
P206	$O + NO \rightarrow N + O_2$	$7.5e-12 * (T_{gas}/300.0)^{*} \exp(-19500.0/T_{gas})$
P207	$O + NO \rightarrow NO_2$	$4.2e-18$
P208	$O + N_2O \rightarrow N_2 + O_2$	$8.3e-12 * \exp(-14000.0/T_{gas})$

Table A1. (Continued.)

No.	Reaction	Rate coefficient
P209	$O + N_2O \rightarrow NO + NO$	$1.5e-10 * exp(-14\ 090.0/T_{gas})$
P210	$O + NO_2 \rightarrow NO + O_2$	$9.1e-12 * (T_{gas}/300.0)^{**0.18}$
P211	$O + NO_3 \rightarrow O_2 + NO_2$	$1.0e-11$
P212	$N_2 + O_2 \rightarrow O + N_2O$	$2.5e-10 * exp(-50\ 390.0/T_{gas})$
P213	$NO + NO \rightarrow N + NO_2$	$3.3e-16 * (300.0/T_{gas})^{**0.5} * exp(-39\ 200.0/T_{gas})$
P214	$NO + NO \rightarrow O + N_2O$	$2.2e-12 * exp(-32\ 100.0/T_{gas})$
P215	$NO + NO \rightarrow N_2 + O_2$	$5.1e-13 * exp(-33\ 660.0/T_{gas})$
P216	$NO + O_2 \rightarrow O + NO_2$	$2.8e-12 * exp(-23\ 400.0/T_{gas})$
P217	$NO + O_3 \rightarrow O_2 + NO_2$	$2.5e-13 * exp(-765.0/T_{gas})$
P218	$NO + N_2O \rightarrow N_2 + NO_2$	$4.6e-10 * exp(-25\ 170.0/T_{gas})$
P219	$NO + NO_3 \rightarrow NO_2 + NO_2$	$1.7e-11$
P220	$O_2 + O_2 \rightarrow O + O_3$	$2.0e-11 * exp(-49\ 800.0/T_{gas})$
P221	$O_2 + NO_2 \rightarrow NO + O_3$	$2.8e-12 * exp(-25\ 400.0/T_{gas})$
P222	$NO_2 + NO_2 \rightarrow NO + NO + O_2$	$3.3e-12 * exp(-13\ 500.0/T_{gas})$
P223	$NO_2 + NO_2 \rightarrow NO + NO_3$	$4.5e-10 * exp(-18\ 500.0/T_{gas})$
P224	$NO_2 + O_3 \rightarrow O_2 + NO_3$	$1.2e-13 * exp(-2\ 450.0/T_{gas})$
P225	$NO_2 + NO_3 \rightarrow NO + NO_2 + O_2$	$2.3e-13 * exp(-1\ 600.0/T_{gas})$
P226	$NO_3 + O_2 \rightarrow NO_2 + O_3$	$1.5e-12 * exp(-15\ 020.0/T_{gas})$
P227	$NO_3 + NO_3 \rightarrow O_2 + NO_2 + NO_2$	$4.3e-12 * exp(-3\ 850.0/T_{gas})$
P228	$N + N \rightarrow N_2^+ + e^-$	$2.7e-11 * exp(-6.74e4/T_{gas})$
P229	$N + O \rightarrow NO^+ + e^-$	$1.6e-12 * (T_{gas}/300.0)^{**0.5} * (0.19 + 8.6 * T_{gas}) * exp(-32\ 000.0/T_{gas})$
P230	$N_2 + N_2 \rightarrow N + N + N_2$	$5.4e-8 * (1.0 - exp(-3\ 354.0/T_{gas})) * exp(-113\ 200.0/T_{gas})^{*1.0}$
P231	$N_2 + O_2 \rightarrow N + N + O_2$	$5.4e-8 * (1.0 - exp(-3\ 354.0/T_{gas})) * exp(-113\ 200.0/T_{gas})^{*1.0}$
P232	$N_2 + NO \rightarrow N + N + NO$	$5.4e-8 * (1.0 - exp(-3\ 354.0/T_{gas})) * exp(-113\ 200.0/T_{gas})^{*1.0}$
P233	$N_2 + O \rightarrow N + N + O$	$5.4e-8 * (1.0 - exp(-3\ 354.0/T_{gas})) * exp(-113\ 200.0/T_{gas})^{*6.6}$
P234	$N_2 + N \rightarrow N + N + N$	$5.4e-8 * (1.0 - exp(-3\ 354.0/T_{gas})) * exp(-113\ 200.0/T_{gas})^{*6.6}$
P235	$O_2 + N_2 \rightarrow O + O + N_2$	$6.1e-9 * (1.0 - exp(-2\ 240.0/T_{gas})) * exp(-59\ 380.0/T_{gas})^{*1.0}$
P236	$O_2 + O_2 \rightarrow O + O + O_2$	$6.1e-9 * (1.0 - exp(-2\ 240.0/T_{gas})) * exp(-59\ 380.0/T_{gas})^{*5.9}$
P237	$O_2 + O \rightarrow O + O + O$	$6.1e-9 * (1.0 - exp(-2\ 240.0/T_{gas})) * exp(-59\ 380.0/T_{gas})^{*21.}$
P238	$O_2 + N \rightarrow O + O + N$	$6.1e-9 * (1.0 - exp(-2\ 240.0/T_{gas})) * exp(-59\ 380.0/T_{gas})^{*1.0}$
P239	$O_2 + NO \rightarrow O + O + NO$	$6.1e-9 * (1.0 - exp(-2\ 240.0/T_{gas})) * exp(-59\ 380.0/T_{gas})^{*1.0}$
P240	$NO + N_2 \rightarrow N + O + N_2$	$8.7e-9 * exp(-75\ 994.0/T_{gas})^{*1.0}$
P241	$NO + O_2 \rightarrow N + O + O_2$	$8.7e-9 * exp(-75\ 994.0/T_{gas})^{*1.0}$
P242	$NO + O \rightarrow N + O + O$	$8.7e-9 * exp(-75\ 994.0/T_{gas})^{*20.}$
P243	$NO + N \rightarrow N + O + N$	$8.7e-9 * exp(-75\ 994.0/T_{gas})^{*20.}$
P244	$NO + NO \rightarrow N + O + NO$	$8.7e-9 * exp(-75\ 994.0/T_{gas})^{*20.}$
P245	$O_3 + N_2 \rightarrow O_2 + O + N_2$	$6.6e-10 * exp(-11\ 600.0/T_{gas})^{*1.0}$
P246	$O_3 + O_2 \rightarrow O_2 + O + O_2$	$6.6e-10 * exp(-11\ 600.0/T_{gas})^{*0.38}$
P247	$O_3 + N \rightarrow O_2 + O + N$	$6.6e-10 * exp(-11\ 600.0/T_{gas})^{*6.3} * exp(170.0/T_{gas})$
P248	$O_3 + O \rightarrow O_2 + O + O$	$6.6e-10 * exp(-11\ 600.0/T_{gas})^{*6.3} * exp(170.0/T_{gas})$
P249	$N_2O + N_2 \rightarrow N_2 + O + N_2$	$1.2e-8 * (300.0/T_{gas}) * exp(-29\ 000.0/T_{gas})^{*1.0}$
P250	$N_2O + O_2 \rightarrow N_2 + O + O_2$	$1.2e-8 * (300.0/T_{gas}) * exp(-29\ 000.0/T_{gas})^{*1.0}$
P251	$N_2O + NO \rightarrow N_2 + O + NO$	$1.2e-8 * (300.0/T_{gas}) * exp(-29\ 000.0/T_{gas})^{*2.0}$
P252	$N_2O + N_2O \rightarrow N_2 + O + N_2O$	$1.2e-8 * (300.0/T_{gas}) * exp(-29\ 000.0/T_{gas})^{*4.0}$
P253	$NO_2 + N_2 \rightarrow NO + O + N_2$	$6.8e-6 * (300.0/T_{gas})^{**2} * exp(-36\ 180.0/T_{gas})^{*1.0}$
P254	$NO_2 + O_2 \rightarrow NO + O + O_2$	$6.8e-6 * (300.0/T_{gas})^{**2} * exp(-36\ 180.0/T_{gas})^{*0.78}$
P255	$NO_2 + NO \rightarrow NO + O + NO$	$6.8e-6 * (300.0/T_{gas})^{**2} * exp(-36\ 180.0/T_{gas})^{*7.8}$
P256	$NO_2 + NO_2 \rightarrow NO + O + NO_2$	$6.8e-6 * (300.0/T_{gas})^{**2} * exp(-36\ 180.0/T_{gas})^{*5.9}$
P257	$NO_3 + N_2 \rightarrow NO_2 + O + N_2$	$3.1e-5 * (300.0/T_{gas})^{**2} * exp(-25\ 000.0/T_{gas})^{*1.0}$
P258	$NO_3 + O_2 \rightarrow NO_2 + O + O_2$	$3.1e-5 * (300.0/T_{gas})^{**2} * exp(-25\ 000.0/T_{gas})^{*1.0}$
P259	$NO_3 + NO \rightarrow NO_2 + O + NO$	$3.1e-5 * (300.0/T_{gas})^{**2} * exp(-25\ 000.0/T_{gas})^{*1.0}$
P260	$NO_3 + N \rightarrow NO_2 + O + N$	$3.1e-5 * (300.0/T_{gas})^{**2} * exp(-25\ 000.0/T_{gas})^{*10.}$
P261	$NO_3 + O \rightarrow NO_2 + O + O$	$3.1e-5 * (300.0/T_{gas})^{**2} * exp(-25\ 000.0/T_{gas})^{*10.}$
P262	$NO_3 + N_2 \rightarrow NO + O_2 + N_2$	$6.2e-5 * (300.0/T_{gas})^{**2} * exp(-25\ 000.0/T_{gas})^{*1.0}$
P263	$NO_3 + O_2 \rightarrow NO + O_2 + O_2$	$6.2e-5 * (300.0/T_{gas})^{**2} * exp(-25\ 000.0/T_{gas})^{*1.0}$
P264	$NO_3 + NO \rightarrow NO + O_2 + NO$	$6.2e-5 * (300.0/T_{gas})^{**2} * exp(-25\ 000.0/T_{gas})^{*1.0}$
P265	$NO_3 + N \rightarrow NO + O_2 + N$	$6.2e-5 * (300.0/T_{gas})^{**2} * exp(-25\ 000.0/T_{gas})^{*12.}$
P266	$NO_3 + O \rightarrow NO + O_2 + O$	$6.2e-5 * (300.0/T_{gas})^{**2} * exp(-25\ 000.0/T_{gas})^{*12.}$

Table A1. (Continued.)

No.	Reaction	Rate coefficient
P267	$\text{N}_2\text{O}_5 + \text{M} \rightarrow \text{NO}_2 + \text{NO}_3 + \text{M}$	$2.1\text{e}-11^*(300.0/\text{Tgas})^{**4.4}\exp(-11080.0/\text{Tgas})$
P268	$\text{N} + \text{N} + \text{N}_2 \rightarrow \text{N}_2 + \text{N}_2$	$\max(8.3\text{e}-34\exp(500.0/\text{Tgas}), 1.91\text{e}-33)$
P269	$\text{N} + \text{N} + \text{O}_2 \rightarrow \text{N}_2 + \text{O}_2$	$1.8\text{e}-33\exp(435.0/\text{Tgas})^{*1.0}$
P270	$\text{N} + \text{N} + \text{NO} \rightarrow \text{N}_2 + \text{NO}$	$1.8\text{e}-33\exp(435.0/\text{Tgas})^{*1.0}$
P271	$\text{N} + \text{N} + \text{N} \rightarrow \text{N}_2 + \text{N}$	$1.8\text{e}-33\exp(435.0/\text{Tgas})^{*3.0}$
P272	$\text{N} + \text{N} + \text{O} \rightarrow \text{N}_2 + \text{O}$	$1.8\text{e}-33\exp(435.0/\text{Tgas})^{*3.0}$
P273	$\text{O} + \text{O} + \text{N}_2 \rightarrow \text{O}_2 + \text{N}_2$	$\max(2.8\text{e}-34\exp(720.0/\text{Tgas}), 1.0\text{e}-33^*(300.0/\text{Tgas})^{**0.41})$
P274	$\text{O} + \text{O} + \text{O}_2 \rightarrow \text{O}_2 + \text{O}_2$	$4.0\text{e}-33^*(300.0/\text{Tgas})^{**0.41*1.0}$
P275	$\text{O} + \text{O} + \text{N} \rightarrow \text{O}_2 + \text{N}$	$4.0\text{e}-33^*(300.0/\text{Tgas})^{**0.41*0.8}$
P276	$\text{O} + \text{O} + \text{O} \rightarrow \text{O}_2 + \text{O}$	$4.0\text{e}-33^*(300.0/\text{Tgas})^{**0.41*3.6}$
P277	$\text{O} + \text{O} + \text{NO} \rightarrow \text{O}_2 + \text{NO}$	$4.0\text{e}-33^*(300.0/\text{Tgas})^{**0.41*0.17}$
P278	$\text{N} + \text{O} + \text{N}_2 \rightarrow \text{NO} + \text{N}_2$	$1.0\text{e}-32^*(300.0/\text{Tgas})^{**0.5}$
P279	$\text{N} + \text{O} + \text{O}_2 \rightarrow \text{NO} + \text{O}_2$	$1.0\text{e}-32^*(300.0/\text{Tgas})^{**0.5}$
P280	$\text{N} + \text{O} + \text{N} \rightarrow \text{NO} + \text{N}$	$1.8\text{e}-31^*(300.0/\text{Tgas})$
P281	$\text{N} + \text{O} + \text{O} \rightarrow \text{NO} + \text{O}$	$1.8\text{e}-31^*(300.0/\text{Tgas})$
P282	$\text{N} + \text{O} + \text{NO} \rightarrow \text{NO} + \text{NO}$	$1.8\text{e}-31^*(300.0/\text{Tgas})$
P283	$\text{O} + \text{O}_2 + \text{N}_2 \rightarrow \text{O}_3 + \text{N}_2$	$\max(5.8\text{e}-34^*(300.0/\text{Tgas})^{**2.8}, 5.4\text{e}-34^*(300.0/\text{Tgas})^{**1.9})$
P284	$\text{O} + \text{O}_2 + \text{O}_2 \rightarrow \text{O}_3 + \text{O}_2$	$7.6\text{e}-34^*(300.0/\text{Tgas})^{**1.9}$
P285	$\text{O} + \text{O}_2 + \text{NO} \rightarrow \text{O}_3 + \text{NO}$	$7.6\text{e}-34^*(300.0/\text{Tgas})^{**1.9}$
P286	$\text{O} + \text{O}_2 + \text{N} \rightarrow \text{O}_3 + \text{N}$	$\min(3.9\text{e}-33^*(300.0/\text{Tgas})^{**1.9}, 1.1\text{e}-34\exp(1060.0/\text{Tgas}))$
P287	$\text{O} + \text{O}_2 + \text{O} \rightarrow \text{O}_3 + \text{O}$	$\min(3.9\text{e}-33^*(300.0/\text{Tgas})^{**1.9}, 1.1\text{e}-34\exp(1060.0/\text{Tgas}))$
P288	$\text{O} + \text{N}_2 + \text{M} \rightarrow \text{N}_2\text{O} + \text{M}$	$3.9\text{e}-35\exp(-10400.0/\text{Tgas})$
P289	$\text{O} + \text{NO} + \text{N}_2 \rightarrow \text{NO}_2 + \text{N}_2$	$1.2\text{e}-31^*(300.0/\text{Tgas})^{**1.8*1.0}$
P290	$\text{O} + \text{NO} + \text{O}_2 \rightarrow \text{NO}_2 + \text{O}_2$	$1.2\text{e}-31^*(300.0/\text{Tgas})^{**1.8*0.78}$
P291	$\text{O} + \text{NO} + \text{NO} \rightarrow \text{NO}_2 + \text{NO}$	$1.2\text{e}-31^*(300.0/\text{Tgas})^{**1.8*0.78}$
P292	$\text{O} + \text{NO}_2 + \text{N}_2 \rightarrow \text{NO}_3 + \text{N}_2$	$8.9\text{e}-32^*(300.0/\text{Tgas})^{**2*1.0}$
P293	$\text{O} + \text{NO}_2 + \text{O}_2 \rightarrow \text{NO}_3 + \text{O}_2$	$8.9\text{e}-32^*(300.0/\text{Tgas})^{**2*1.0}$
P294	$\text{O} + \text{NO}_2 + \text{N} \rightarrow \text{NO}_3 + \text{N}$	$8.9\text{e}-32^*(300.0/\text{Tgas})^{**2*13.}$
P295	$\text{O} + \text{NO}_2 + \text{O} \rightarrow \text{NO}_3 + \text{O}$	$8.9\text{e}-32^*(300.0/\text{Tgas})^{**2*13.}$
P296	$\text{O} + \text{NO}_2 + \text{NO} \rightarrow \text{NO}_3 + \text{NO}$	$8.9\text{e}-32^*(300.0/\text{Tgas})^{**2*2.4}$
P297	$\text{NO}_2 + \text{NO}_3 + \text{M} \rightarrow \text{N}_2\text{O}_5 + \text{M}$	$3.7\text{e}-30^*(300.0/\text{Tgas})^{**4.1}$
P298	$\text{N}^+ + \text{O} \rightarrow \text{N} + \text{O}^+$	$1.0\text{e}-12$
P299	$\text{N}^+ + \text{O}_2 \rightarrow \text{O}_2^+ + \text{N}$	$2.8\text{e}-10$
P300	$\text{N}^+ + \text{O}_2 \rightarrow \text{NO}^+ + \text{O}$	$2.5\text{e}-10$
P301	$\text{N}^+ + \text{O}_2 \rightarrow \text{O}^+ + \text{NO}$	$2.8\text{e}-11$
P302	$\text{N}^+ + \text{O}_3 \rightarrow \text{NO}^+ + \text{O}_2$	$5.0\text{e}-10$
P303	$\text{N}^+ + \text{NO} \rightarrow \text{NO}^+ + \text{N}$	$8.0\text{e}-10$
P304	$\text{N}^+ + \text{NO} \rightarrow \text{N}_2^+ + \text{O}$	$3.0\text{e}-12$
P305	$\text{N}^+ + \text{NO} \rightarrow \text{O}^+ + \text{N}_2$	$1.0\text{e}-12$
P306	$\text{N}^+ + \text{N}_2\text{O} \rightarrow \text{NO}^+ + \text{N}_2$	$5.5\text{e}-10$
P307	$\text{O}^+ + \text{N}_2 \rightarrow \text{NO}^+ + \text{N}$	$(1.5-2.0\text{e}-3^*\text{TeffN} + 9.6\text{e}-7^*\text{TeffN}^{**2})^{*1.0\text{e}-12}$
P308	$\text{O}^+ + \text{O}_2 \rightarrow \text{O}_2^+ + \text{O}$	$2.0\text{e}-11^*(300.0/\text{TeffN})^{**0.5}$
P309	$\text{O}^+ + \text{O}_3 \rightarrow \text{O}_2^+ + \text{O}_2$	$1.0\text{e}-10$
P310	$\text{O}^+ + \text{NO} \rightarrow \text{NO}^+ + \text{O}$	$2.4\text{e}-11$
P311	$\text{O}^+ + \text{NO} \rightarrow \text{O}_2^+ + \text{N}$	$3.0\text{e}-12$
P312	$\text{O}^+ + \text{N}^{(2)\text{D}} \rightarrow \text{N}^+ + \text{O}$	$1.3\text{e}-10$
P313	$\text{O}^+ + \text{N}_2\text{O} \rightarrow \text{NO}^+ + \text{NO}$	$2.3\text{e}-10$
P314	$\text{O}^+ + \text{N}_2\text{O} \rightarrow \text{N}_2\text{O}^+ + \text{O}$	$2.2\text{e}-10$
P315	$\text{O}^+ + \text{N}_2\text{O} \rightarrow \text{O}_2^+ + \text{N}_2$	$2.0\text{e}-11$
P316	$\text{O}^+ + \text{NO}_2 \rightarrow \text{NO}_2^+ + \text{O}$	$1.6\text{e}-9$
P317	$\text{N}_2^+ + \text{O}_2 \rightarrow \text{O}_2^+ + \text{N}_2$	$6.0\text{e}-11^*(300.0/\text{TeffN2})^{**0.5}$
P318	$\text{N}_2^+ + \text{O} \rightarrow \text{NO}^+ + \text{N}$	$1.3\text{e}-10^*(300.0/\text{TeffN2})^{**0.5}$
P319	$\text{N}_2^+ + \text{O}_3 \rightarrow \text{O}_2^+ + \text{O} + \text{N}_2$	$1.0\text{e}-10$
P320	$\text{N}_2^+ + \text{N} \rightarrow \text{N}^+ + \text{N}_2$	$7.2\text{e}-13^*(\text{TeffN2}/300.0)$
P321	$\text{N}_2^+ + \text{NO} \rightarrow \text{NO}^+ + \text{N}_2$	$3.3\text{e}-10$
P322	$\text{N}_2^+ + \text{N}_2\text{O} \rightarrow \text{N}_2\text{O}^+ + \text{N}_2$	$5.0\text{e}-10$
P323	$\text{N}_2^+ + \text{N}_2\text{O} \rightarrow \text{NO}^+ + \text{N} + \text{N}_2$	$4.0\text{e}-10$
P324	$\text{N}_2^+(\text{B}^2) + \text{O}_2 \rightarrow \text{O}_2^+ + \text{N}_2$	$6.0\text{e}-11^*(300.0/\text{TeffN2})^{**0.5}$

Table A1. (Continued.)

No.	Reaction	Rate coefficient
P325	$\text{N}_2^+(\text{B}^2) + \text{O} \rightarrow \text{NO}^+ + \text{N}$	$1.3\text{e-}10^* (300.0/\text{TeffN}2)^{**0.5}$
P326	$\text{N}_2^+(\text{B}^2) + \text{O}_3 \rightarrow \text{O}_2^+ + \text{O} + \text{N}_2$	$1.0\text{e-}10$
P327	$\text{N}_2^+(\text{B}^2) + \text{N} \rightarrow \text{N}^+ + \text{N}_2$	$7.2\text{e-}13^* (\text{TeffN}2/300.0)$
P328	$\text{N}_2^+(\text{B}^2) + \text{NO} \rightarrow \text{NO}^+ + \text{N}_2$	$3.3\text{e-}10$
P329	$\text{N}_2^+(\text{B}^2) + \text{N}_2\text{O} \rightarrow \text{N}_2\text{O}^+ + \text{N}_2$	$5.0\text{e-}10$
P330	$\text{N}_2^+(\text{B}^2) + \text{N}_2\text{O} \rightarrow \text{NO}^+ + \text{N} + \text{N}_2$	$4.0\text{e-}10$
P331	$\text{N}_2^+(\text{B}^2) + \text{N}_2 \rightarrow \text{N}_2^+ + \text{N}_2$	$8.8\text{e-}10$
P332	$\text{N}_2^+(\text{B}^2) + \text{O}_2 \rightarrow \text{N}_2^+ + \text{O} + \text{O}^{(1S)}$	$1.0\text{e-}9$
P333	$\text{O}_2^+ + \text{N}_2 \rightarrow \text{NO}^+ + \text{NO}$	$1.0\text{e-}17$
P334	$\text{O}_2^+ + \text{N} \rightarrow \text{NO}^+ + \text{O}$	$1.2\text{e-}10$
P335	$\text{O}_2^+ + \text{NO} \rightarrow \text{NO}^+ + \text{O}_2$	$6.3\text{e-}10$
P336	$\text{O}_2^+ + \text{NO}_2 \rightarrow \text{NO}^+ + \text{O}_3$	$1.0\text{e-}11$
P337	$\text{O}_2^+ + \text{NO}_2 \rightarrow \text{NO}_2^+ + \text{O}_2$	$6.6\text{e-}10$
P338	$\text{N}_3^+ + \text{O}_2 \rightarrow \text{O}_2^+ + \text{N} + \text{N}_2$	$2.3\text{e-}11$
P339	$\text{N}_3^+ + \text{O}_2 \rightarrow \text{NO}_2^+ + \text{N}_2$	$4.4\text{e-}11$
P340	$\text{N}_3^+ + \text{N} \rightarrow \text{N}_2^+ + \text{N}_2$	$6.6\text{e-}11$
P341	$\text{N}_3^+ + \text{NO} \rightarrow \text{NO}^+ + \text{N} + \text{N}_2$	$7.0\text{e-}11$
P342	$\text{N}_3^+ + \text{NO} \rightarrow \text{N}_2\text{O}^+ + \text{N}_2$	$7.0\text{e-}11$
P343	$\text{NO}_2^+ + \text{NO} \rightarrow \text{NO}^+ + \text{NO}_2$	$2.9\text{e-}10$
P344	$\text{N}_2\text{O}^+ + \text{NO} \rightarrow \text{NO}^+ + \text{N}_2\text{O}$	$2.9\text{e-}10$
P345	$\text{N}_4^+ + \text{N}_2 \rightarrow \text{N}_2^+ + \text{N}_2 + \text{N}_2$	$\min(2.1\text{e-}16^* \exp(\text{TeffN}4/121.0), 1.0\text{e-}10)$
P346	$\text{N}_4^+ + \text{O}_2 \rightarrow \text{O}_2^+ + \text{N}_2 + \text{N}_2$	$2.5\text{e-}10$
P347	$\text{N}_4^+ + \text{O} \rightarrow \text{O}^+ + \text{N}_2 + \text{N}_2$	$2.5\text{e-}10$
P348	$\text{N}_4^+ + \text{N} \rightarrow \text{N}^+ + \text{N}_2 + \text{N}_2$	$1.0\text{e-}11$
P349	$\text{N}_4^+ + \text{NO} \rightarrow \text{NO}^+ + \text{N}_2 + \text{N}_2$	$4.0\text{e-}10$
P350	$\text{O}_4^+ + \text{N}_2 \rightarrow \text{O}_2^+ \text{N}_2 + \text{O}_2$	$4.6\text{e-}12^* (\text{TeffN}4/300.0)^{**2.5} \exp(-2650.0/\text{TeffN}4)$
P351	$\text{O}_4^+ + \text{O}_2 \rightarrow \text{O}_2^+ + \text{O}_2 + \text{O}_2$	$3.3\text{e-}6^* (300.0/\text{TeffN}4)^{**4} \exp(-5030.0/\text{TeffN}4)$
P352	$\text{O}_4^+ + \text{O}_2(a^1) \rightarrow \text{O}_2^+ + \text{O}_2 + \text{O}_2$	$1.0\text{e-}10$
P353	$\text{O}_4^+ + \text{O}_2(b^1) \rightarrow \text{O}_2^+ + \text{O}_2 + \text{O}_2$	$1.0\text{e-}10$
P354	$\text{O}_4^+ + \text{O} \rightarrow \text{O}_2^+ + \text{O}_3$	$3.0\text{e-}10$
P355	$\text{O}_4^+ + \text{NO} \rightarrow \text{NO}^+ + \text{O}_2 + \text{O}_2$	$1.0\text{e-}10$
P356	$\text{O}_2^+ \text{N}_2 + \text{N}_2 \rightarrow \text{O}_2^+ + \text{N}_2 + \text{N}_2$	$1.1\text{e-}6^* (300.0/\text{TeffN}4)^{**5.3} \exp(-2360.0/\text{TeffN}4)$
P357	$\text{O}_2^+ \text{N}_2 + \text{O}_2 \rightarrow \text{O}_4^+ + \text{N}_2$	$1.0\text{e-}9$
P358	$\text{N}^+ + \text{N}_2 + \text{N}_2 \rightarrow \text{N}_3^+ + \text{N}_2$	$1.7\text{e-}29^* (300.0/\text{TeffN})^{**2.1}$
P359	$\text{N}^+ + \text{O} + \text{M} \rightarrow \text{NO}^+ + \text{M}$	$1.0\text{e-}29$
P360	$\text{N}^+ + \text{N} + \text{M} \rightarrow \text{N}_2^+ + \text{M}$	$1.0\text{e-}29$
P361	$\text{O}^+ + \text{N}_2 + \text{M} \rightarrow \text{NO}^+ + \text{N} + \text{M}$	$6.0\text{e-}29^* (300.0/\text{TeffN})^{**2}$
P362	$\text{O}^+ + \text{O} + \text{M} \rightarrow \text{O}_2^+ + \text{M}$	$1.0\text{e-}29$
P363	$\text{O}^+ + \text{N} + \text{M} \rightarrow \text{NO}^+ + \text{M}$	$1.0\text{e-}29$
P364	$\text{N}_2^+ + \text{N}_2 + \text{N}_2 \rightarrow \text{N}_4^+ + \text{N}_2$	$5.2\text{e-}29^* (300.0/\text{TeffN}2)^{**2.2}$
P365	$\text{N}_2^+ + \text{N} + \text{N}_2 \rightarrow \text{N}_3^+ + \text{N}_2$	$9.0\text{e-}30 \exp(400.0/\text{TeffN}2)$
P366	$\text{N}_2^+(\text{B}^2) + \text{N}_2 + \text{N}_2 \rightarrow \text{N}_4^+ + \text{N}_2$	$6.2\text{e-}29^* (300.0/\text{TeffN}3Q)^{**1.7}$
P367	$\text{N}_2^+(\text{B}^2) + \text{N} + \text{N}_2 \rightarrow \text{N}_3^+ + \text{N}_2$	$9.0\text{e-}30 \exp(400.0/\text{TeffN}2)$
P368	$\text{O}_2^+ + \text{O}_2 + \text{O}_2 \rightarrow \text{O}_4^+ + \text{O}_2$	$2.4\text{e-}30^* (300.0/\text{TeffN}2)^{**3.2}$
P369	$\text{O}_2^+ + \text{N}_2 + \text{N}_2 \rightarrow \text{O}_2^+ \text{N}_2 + \text{N}_2$	$9.0\text{e-}31^* (300.0/\text{TeffN}2)^{**2}$
P370	$\text{O}^- + \text{O}_2(a^1) \rightarrow \text{O}_2^- + \text{O}$	$1.0\text{e-}10$
P371	$\text{O}^- + \text{O}_3 \rightarrow \text{O}_3^- + \text{O}$	$8.0\text{e-}10$
P372	$\text{O}^- + \text{NO}_2 \rightarrow \text{NO}_2^- + \text{O}$	$1.2\text{e-}9$
P373	$\text{O}^- + \text{N}_2\text{O} \rightarrow \text{NO}^- + \text{NO}$	$2.0\text{e-}10$
P374	$\text{O}^- + \text{N}_2\text{O} \rightarrow \text{N}_2\text{O}^- + \text{O}$	$2.0\text{e-}12$
P375	$\text{O}_2^- + \text{O} \rightarrow \text{O}^- + \text{O}_2$	$3.3\text{e-}10$
P376	$\text{O}_2^- + \text{O}_3 \rightarrow \text{O}_3^- + \text{O}_2$	$3.5\text{e-}10$
P377	$\text{O}_2^- + \text{NO}_2 \rightarrow \text{NO}_2^- + \text{O}_2$	$7.0\text{e-}10$
P378	$\text{O}_2^- + \text{NO}_3 \rightarrow \text{NO}_3^- + \text{O}_2$	$5.0\text{e-}10$
P379	$\text{O}_3^- + \text{O} \rightarrow \text{O}_2^- + \text{O}_2$	$1.0\text{e-}11$
P380	$\text{O}_3^- + \text{NO} \rightarrow \text{NO}_3^- + \text{O}$	$1.0\text{e-}11$
P381	$\text{O}_3^- + \text{NO} \rightarrow \text{NO}_2^- + \text{O}_2$	$2.6\text{e-}12$

Table A1. (Continued.)

No.	Reaction	Rate coefficient
P382	$O_3^- + NO_2 \rightarrow NO_2^- + O_3$	7.0e-11
P383	$O_3^- + NO_2 \rightarrow NO_3^- + O_2$	2.0e-11
P384	$O_3^- + NO_3 \rightarrow NO_3^- + O_3$	5.0e-10
P385	$NO^- + O_2 \rightarrow O_2^- + NO$	5.0e-10
P386	$NO^- + NO_2 \rightarrow NO_2^- + NO$	7.4e-10
P387	$NO^- + N_2O \rightarrow NO_2^- + N_2$	2.8e-14
P388	$NO_2^- + O_3 \rightarrow NO_3^- + O_2$	1.8e-11
P389	$NO_2^- + NO_2 \rightarrow NO_3^- + NO$	4.0e-12
P390	$NO_2^- + NO_3 \rightarrow NO_3^- + NO_2$	5.0e-10
P391	$NO_2^- + N_2O_5 \rightarrow NO_3^- + NO_2 + NO_2$	7.0e-10
P392	$NO_3^- + NO \rightarrow NO_2^- + NO_2$	3.0e-15
P393	$O_4^- + N_2 \rightarrow O_2^- + O_2 + N_2$	$1.0e-10^* \exp(-1044.0/TeffN)$
P394	$O_4^- + O_2 \rightarrow O_2^- + O_2 + O_2$	$1.0e-10^* \exp(-1044.0/TeffN)$
P395	$O_4^- + O \rightarrow O_3^- + O_2$	4.0e-10
P396	$O_4^- + O \rightarrow O^- + O_2 + O_2$	3.0e-10
P397	$O_4^- + O_2(a^1) \rightarrow O_2^- + O_2 + O_2$	1.0e-10
P398	$O_4^- + O_2(b^1) \rightarrow O_2^- + O_2 + O_2$	1.0e-10
P399	$O_4^- + NO \rightarrow NO_3^- + O_2$	2.5e-10
P400	$O^- + O_2 + M \rightarrow O_3^- + M$	$1.1e-30^*(300.0/TeffN)$
P401	$O^- + NO + M \rightarrow NO_2^- + M$	1.0e-29
P402	$O_2^- + O_2 + M \rightarrow O_4^- + M$	$3.5e-31^*(300.0/TeffN2)$
P403	$O^- + N^+ \rightarrow O + N$	$2.0e-7^*(300.0/TionN)**0.5$
P404	$O^- + N_2^+ \rightarrow O + N_2$	$2.0e-7^*(300.0/TionN)**0.5$
P405	$O^- + O^+ \rightarrow O + O$	$2.0e-7^*(300.0/TionN)**0.5$
P406	$O^- + O_2^+ \rightarrow O + O_2$	$2.0e-7^*(300.0/TionN)**0.5$
P407	$O^- + NO^+ \rightarrow O + NO$	$2.0e-7^*(300.0/TionN)**0.5$
P408	$O^- + N_2O^+ \rightarrow O + N_2O$	$2.0e-7^*(300.0/TionN)**0.5$
P409	$O^- + NO_2^+ \rightarrow O + NO_2$	$2.0e-7^*(300.0/TionN)**0.5$
P410	$O^- + N_2^+(B^2) \rightarrow O + N_2$	$2.0e-7^*(300.0/TionN)**0.5$
P411	$O_2^- + N^+ \rightarrow O_2 + N$	$2.0e-7^*(300.0/TionN)**0.5$
P412	$O_2^- + N_2^+ \rightarrow O_2 + N_2$	$2.0e-7^*(300.0/TionN)**0.5$
P413	$O_2^- + O^+ \rightarrow O_2 + O$	$2.0e-7^*(300.0/TionN)**0.5$
P414	$O_2^- + O_2^+ \rightarrow O_2 + O_2$	$2.0e-7^*(300.0/TionN)**0.5$
P415	$O_2^- + NO^+ \rightarrow O_2 + NO$	$2.0e-7^*(300.0/TionN)**0.5$
P416	$O_2^- + N_2O^+ \rightarrow O_2 + N_2O$	$2.0e-7^*(300.0/TionN)**0.5$
P417	$O_2^- + NO_2^+ \rightarrow O_2 + NO_2$	$2.0e-7^*(300.0/TionN)**0.5$
P418	$O_2^- + N_2^+(B^2) \rightarrow O_2 + N_2$	$2.0e-7^*(300.0/TionN)**0.5$
P419	$O_3^- + N^+ \rightarrow O_3 + N$	$2.0e-7^*(300.0/TionN)**0.5$
P420	$O_3^- + N_2^+ \rightarrow O_3 + N_2$	$2.0e-7^*(300.0/TionN)**0.5$
P421	$O_3^- + O^+ \rightarrow O_3 + O$	$2.0e-7^*(300.0/TionN)**0.5$
P422	$O_3^- + O_2^+ \rightarrow O_3 + O_2$	$2.0e-7^*(300.0/TionN)**0.5$
P423	$O_3^- + NO^+ \rightarrow O_3 + NO$	$2.0e-7^*(300.0/TionN)**0.5$
P424	$O_3^- + N_2O^+ \rightarrow O_3 + N_2O$	$2.0e-7^*(300.0/TionN)**0.5$
P425	$O_3^- + NO_2^+ \rightarrow O_3 + NO_2$	$2.0e-7^*(300.0/TionN)**0.5$
P426	$O_3^- + N_2^+(B^2) \rightarrow O_3 + N_2$	$2.0e-7^*(300.0/TionN)**0.5$
P427	$NO^- + N^+ \rightarrow NO + N$	$2.0e-7^*(300.0/TionN)**0.5$
P428	$NO^- + N_2^+ \rightarrow NO + N_2$	$2.0e-7^*(300.0/TionN)**0.5$
P429	$NO^- + O^+ \rightarrow NO + O$	$2.0e-7^*(300.0/TionN)**0.5$
P430	$NO^- + O_2^+ \rightarrow NO + O_2$	$2.0e-7^*(300.0/TionN)**0.5$
P431	$NO^- + NO^+ \rightarrow NO + NO$	$2.0e-7^*(300.0/TionN)**0.5$
P432	$NO^- + N_2O^+ \rightarrow NO + N_2O$	$2.0e-7^*(300.0/TionN)**0.5$
P433	$NO^- + NO_2^+ \rightarrow NO + NO_2$	$2.0e-7^*(300.0/TionN)**0.5$
P434	$NO^- + N_2^+(B^2) \rightarrow NO + N_2$	$2.0e-7^*(300.0/TionN)**0.5$
P435	$NO^- + N^+ \rightarrow NO + N$	$2.0e-7^*(300.0/TionN)**0.5$
P436	$NO^- + N_2^+ \rightarrow NO + N_2$	$2.0e-7^*(300.0/TionN)**0.5$
P437	$NO^- + O^+ \rightarrow NO + O$	$2.0e-7^*(300.0/TionN)**0.5$
P438	$NO^- + O_2^+ \rightarrow NO + O_2$	$2.0e-7^*(300.0/TionN)**0.5$

Table A1. (Continued.)

No.	Reaction	Rate coefficient
P439	$\text{NO}^- + \text{NO}^+ \rightarrow \text{NO} + \text{NO}$	$2.0\text{e-}7^*(300.0/\text{TionN})^{**0.5}$
P440	$\text{NO}^- + \text{N}_2\text{O}^+ \rightarrow \text{NO} + \text{N}_2\text{O}$	$2.0\text{e-}7^*(300.0/\text{TionN})^{**0.5}$
P441	$\text{NO}^- + \text{NO}_2^+ \rightarrow \text{NO} + \text{NO}_2$	$2.0\text{e-}7^*(300.0/\text{TionN})^{**0.5}$
P442	$\text{NO}^- + \text{N}_2^+(\text{B}^2) \rightarrow \text{NO} + \text{N}_2$	$2.0\text{e-}7^*(300.0/\text{TionN})^{**0.5}$
P443	$\text{NO}^- + \text{N}^+ \rightarrow \text{NO} + \text{N}$	$2.0\text{e-}7^*(300.0/\text{TionN})^{**0.5}$
P444	$\text{NO}^- + \text{N}_2^+ \rightarrow \text{NO} + \text{N}_2$	$2.0\text{e-}7^*(300.0/\text{TionN})^{**0.5}$
P445	$\text{NO}^- + \text{O}^+ \rightarrow \text{NO} + \text{O}$	$2.0\text{e-}7^*(300.0/\text{TionN})^{**0.5}$
P446	$\text{NO}^- + \text{O}_2^+ \rightarrow \text{NO} + \text{O}_2$	$2.0\text{e-}7^*(300.0/\text{TionN})^{**0.5}$
P447	$\text{NO}^- + \text{NO}^+ \rightarrow \text{NO} + \text{NO}$	$2.0\text{e-}7^*(300.0/\text{TionN})^{**0.5}$
P448	$\text{NO}^- + \text{N}_2\text{O}^+ \rightarrow \text{NO} + \text{N}_2\text{O}$	$2.0\text{e-}7^*(300.0/\text{TionN})^{**0.5}$
P449	$\text{NO}^- + \text{NO}_2^+ \rightarrow \text{NO} + \text{NO}_2$	$2.0\text{e-}7^*(300.0/\text{TionN})^{**0.5}$
P450	$\text{NO}^- + \text{N}_2^+(\text{B}^2) \rightarrow \text{NO} + \text{N}_2$	$2.0\text{e-}7^*(300.0/\text{TionN})^{**0.5}$
P451	$\text{N}_2\text{O}^- + \text{N}^+ \rightarrow \text{N}_2\text{O} + \text{N}$	$2.0\text{e-}7^*(300.0/\text{TionN})^{**0.5}$
P452	$\text{N}_2\text{O}^- + \text{N}_2^+ \rightarrow \text{N}_2\text{O} + \text{N}_2$	$2.0\text{e-}7^*(300.0/\text{TionN})^{**0.5}$
P453	$\text{N}_2\text{O}^- + \text{O}^+ \rightarrow \text{N}_2\text{O} + \text{O}$	$2.0\text{e-}7^*(300.0/\text{TionN})^{**0.5}$
P454	$\text{N}_2\text{O}^- + \text{O}_2^+ \rightarrow \text{N}_2\text{O} + \text{O}_2$	$2.0\text{e-}7^*(300.0/\text{TionN})^{**0.5}$
P455	$\text{N}_2\text{O}^- + \text{NO}^+ \rightarrow \text{N}_2\text{O} + \text{NO}$	$2.0\text{e-}7^*(300.0/\text{TionN})^{**0.5}$
P456	$\text{N}_2\text{O}^- + \text{N}_2\text{O}^+ \rightarrow \text{N}_2\text{O} + \text{N}_2\text{O}$	$2.0\text{e-}7^*(300.0/\text{TionN})^{**0.5}$
P457	$\text{N}_2\text{O}^- + \text{NO}_2^+ \rightarrow \text{N}_2\text{O} + \text{NO}_2$	$2.0\text{e-}7^*(300.0/\text{TionN})^{**0.5}$
P458	$\text{N}_2\text{O}^- + \text{N}_2^+(\text{B}^2) \rightarrow \text{N}_2\text{O} + \text{N}_2$	$2.0\text{e-}7^*(300.0/\text{TionN})^{**0.5}$
P459	$\text{NO}_2^- + \text{N}^+ \rightarrow \text{NO}_2 + \text{N}$	$2.0\text{e-}7^*(300.0/\text{TionN})^{**0.5}$
P460	$\text{NO}_2^- + \text{N}_2^+ \rightarrow \text{NO}_2 + \text{N}_2$	$2.0\text{e-}7^*(300.0/\text{TionN})^{**0.5}$
P461	$\text{NO}_2^- + \text{O}^+ \rightarrow \text{NO}_2 + \text{O}$	$2.0\text{e-}7^*(300.0/\text{TionN})^{**0.5}$
P462	$\text{NO}_2^- + \text{O}_2^+ \rightarrow \text{NO}_2 + \text{O}_2$	$2.0\text{e-}7^*(300.0/\text{TionN})^{**0.5}$
P463	$\text{NO}_2^- + \text{NO}^+ \rightarrow \text{NO}_2 + \text{NO}$	$2.0\text{e-}7^*(300.0/\text{TionN})^{**0.5}$
P464	$\text{NO}_2^- + \text{N}_2\text{O}^+ \rightarrow \text{NO}_2 + \text{N}_2\text{O}$	$2.0\text{e-}7^*(300.0/\text{TionN})^{**0.5}$
P465	$\text{NO}_2^- + \text{NO}_2^+ \rightarrow \text{NO}_2 + \text{NO}_2$	$2.0\text{e-}7^*(300.0/\text{TionN})^{**0.5}$
P466	$\text{NO}_2^- + \text{N}_2^+(\text{B}^2) \rightarrow \text{NO}_2 + \text{N}_2$	$2.0\text{e-}7^*(300.0/\text{TionN})^{**0.5}$
P467	$\text{NO}_3^- + \text{N}^+ \rightarrow \text{NO}_3 + \text{N}$	$2.0\text{e-}7^*(300.0/\text{TionN})^{**0.5}$
P468	$\text{NO}_3^- + \text{N}_2^+ \rightarrow \text{NO}_3 + \text{N}_2$	$2.0\text{e-}7^*(300.0/\text{TionN})^{**0.5}$
P469	$\text{NO}_3^- + \text{O}^+ \rightarrow \text{NO}_3 + \text{O}$	$2.0\text{e-}7^*(300.0/\text{TionN})^{**0.5}$
P470	$\text{NO}_3^- + \text{O}_2^+ \rightarrow \text{NO}_3 + \text{O}_2$	$2.0\text{e-}7^*(300.0/\text{TionN})^{**0.5}$
P471	$\text{NO}_3^- + \text{NO}^+ \rightarrow \text{NO}_3 + \text{NO}$	$2.0\text{e-}7^*(300.0/\text{TionN})^{**0.5}$
P472	$\text{NO}_3^- + \text{N}_2\text{O}^+ \rightarrow \text{NO}_3 + \text{N}_2\text{O}$	$2.0\text{e-}7^*(300.0/\text{TionN})^{**0.5}$
P473	$\text{NO}_3^- + \text{NO}_2^+ \rightarrow \text{NO}_3 + \text{NO}_2$	$2.0\text{e-}7^*(300.0/\text{TionN})^{**0.5}$
P474	$\text{NO}_3^- + \text{N}_2^+(\text{B}^2) \rightarrow \text{NO}_3 + \text{N}_2$	$2.0\text{e-}7^*(300.0/\text{TionN})^{**0.5}$
P475	$\text{O}^- + \text{N}_2^+ \rightarrow \text{O} + \text{N} + \text{N}$	$1.0\text{e-}7$
P476	$\text{O}^- + \text{N}_3^+ \rightarrow \text{O} + \text{N} + \text{N}_2$	$1.0\text{e-}7$
P477	$\text{O}^- + \text{N}_4^+ \rightarrow \text{O} + \text{N}_2 + \text{N}_2$	$1.0\text{e-}7$
P478	$\text{O}^- + \text{O}_2^+ \rightarrow \text{O} + \text{O} + \text{O}$	$1.0\text{e-}7$
P479	$\text{O}^- + \text{O}_4^+ \rightarrow \text{O} + \text{O}_2 + \text{O}_2$	$1.0\text{e-}7$
P480	$\text{O}^- + \text{NO}^+ \rightarrow \text{O} + \text{N} + \text{O}$	$1.0\text{e-}7$
P481	$\text{O}^- + \text{N}_2\text{O}^+ \rightarrow \text{O} + \text{N}_2 + \text{O}$	$1.0\text{e-}7$
P482	$\text{O}^- + \text{NO}_2^+ \rightarrow \text{O} + \text{N} + \text{O}_2$	$1.0\text{e-}7$
P483	$\text{O}^- + \text{O}_2^+ \text{N}_2 \rightarrow \text{O} + \text{O}_2 + \text{N}_2$	$1.0\text{e-}7$
P484	$\text{O}^- + \text{N}_2^+(\text{B}^2) \rightarrow \text{O} + \text{N} + \text{N}$	$1.0\text{e-}7$
P485	$\text{O}_2^- + \text{N}_2^+ \rightarrow \text{O}_2 + \text{N} + \text{N}$	$1.0\text{e-}7$
P486	$\text{O}_2^- + \text{N}_3^+ \rightarrow \text{O}_2 + \text{N} + \text{N}_2$	$1.0\text{e-}7$
P487	$\text{O}_2^- + \text{N}_4^+ \rightarrow \text{O}_2 + \text{N}_2 + \text{N}_2$	$1.0\text{e-}7$
P488	$\text{O}_2^- + \text{O}_2^+ \rightarrow \text{O}_2 + \text{O} + \text{O}$	$1.0\text{e-}7$
P489	$\text{O}_2^- + \text{O}_4^+ \rightarrow \text{O}_2 + \text{O}_2 + \text{O}_2$	$1.0\text{e-}7$
P490	$\text{O}_2^- + \text{NO}^+ \rightarrow \text{O}_2 + \text{N} + \text{O}$	$1.0\text{e-}7$
P491	$\text{O}_2^- + \text{N}_2\text{O}^+ \rightarrow \text{O}_2 + \text{N}_2 + \text{O}$	$1.0\text{e-}7$
P492	$\text{O}_2^- + \text{NO}_2^+ \rightarrow \text{O}_2 + \text{N} + \text{O}_2$	$1.0\text{e-}7$
P493	$\text{O}_2^- + \text{O}_2^+ \text{N}_2 \rightarrow \text{O}_2 + \text{O}_2 + \text{N}_2$	$1.0\text{e-}7$
P494	$\text{O}_2^- + \text{N}_2^+(\text{B}^2) \rightarrow \text{O}_2 + \text{N} + \text{N}$	$1.0\text{e-}7$
P495	$\text{O}_3^- + \text{N}_2^+ \rightarrow \text{O}_3 + \text{N} + \text{N}$	$1.0\text{e-}7$

Table A1. (Continued.)

No.	Reaction	Rate coefficient
P496	$O_3^- + N_3^+ \rightarrow O_3 + N + N_2$	1.0e-7
P497	$O_3^- + N_4^+ \rightarrow O_3 + N_2 + N_2$	1.0e-7
P498	$O_3^- + O_2^+ \rightarrow O_3 + O + O$	1.0e-7
P499	$O_3^- + O_4^+ \rightarrow O_3 + O_2 + O_2$	1.0e-7
P500	$O_3^- + NO^+ \rightarrow O_3 + N + O$	1.0e-7
P501	$O_3^- + N_2O^+ \rightarrow O_3 + N_2 + O$	1.0e-7
P502	$O_3^- + NO_2^+ \rightarrow O_3 + N + O_2$	1.0e-7
P503	$O_3^- + O_2^+ N_2 \rightarrow O_3 + O_2 + N_2$	1.0e-7
P504	$O_3^- + N_2^+(B^2) \rightarrow O_3 + N + N$	1.0e-7
P505	$NO^- + N_2^+ \rightarrow NO + N + N$	1.0e-7
P506	$NO^- + N_3^+ \rightarrow NO + N + N_2$	1.0e-7
P507	$NO^- + N_4^+ \rightarrow NO + N_2 + N_2$	1.0e-7
P508	$NO^- + O_2^+ \rightarrow NO + O + O$	1.0e-7
P509	$NO^- + O_4^+ \rightarrow NO + O_2 + O_2$	1.0e-7
P510	$NO^- + NO^+ \rightarrow NO + N + O$	1.0e-7
P511	$NO^- + N_2O^+ \rightarrow NO + N_2 + O$	1.0e-7
P512	$NO^- + NO_2^+ \rightarrow NO + N + O_2$	1.0e-7
P513	$NO^- + O_2^+ N_2 \rightarrow NO + O_2 + N_2$	1.0e-7
P514	$NO^- + N_2^+(B^2) \rightarrow NO + N + N$	1.0e-7
P515	$N_2O^- + N_2^+ \rightarrow N_2O + N + N$	1.0e-7
P516	$N_2O^- + N_3^+ \rightarrow N_2O + N + N_2$	1.0e-7
P517	$N_2O^- + N_4^+ \rightarrow N_2O + N_2 + N_2$	1.0e-7
P518	$N_2O^- + O_2^+ \rightarrow N_2O + O + O$	1.0e-7
P519	$N_2O^- + O_4^+ \rightarrow N_2O + O_2 + O_2$	1.0e-7
P520	$N_2O^- + NO^+ \rightarrow N_2O + N + O$	1.0e-7
P521	$N_2O^- + N_2O^+ \rightarrow N_2O + N_2 + O$	1.0e-7
P522	$N_2O^- + NO_2^+ \rightarrow N_2O + N + O_2$	1.0e-7
P523	$N_2O^- + O_2^+ N_2 \rightarrow N_2O + O_2 + N_2$	1.0e-7
P524	$N_2O^- + N_2^+(B^2) \rightarrow N_2O + N + N$	1.0e-7
P525	$NO_2^- + N_2^+ \rightarrow NO_2 + N + N$	1.0e-7
P526	$NO_2^- + N_3^+ \rightarrow NO_2 + N + N_2$	1.0e-7
P527	$NO_2^- + N_4^+ \rightarrow NO_2 + N_2 + N_2$	1.0e-7
P528	$NO_2^- + O_2^+ \rightarrow NO_2 + O + O$	1.0e-7
P529	$NO_2^- + O_4^+ \rightarrow NO_2 + O_2 + O_2$	1.0e-7
P530	$NO_2^- + NO^+ \rightarrow NO_2 + N + O$	1.0e-7
P531	$NO_2^- + N_2O^+ \rightarrow NO_2 + N_2 + O$	1.0e-7
P532	$NO_2^- + NO_2^+ \rightarrow NO_2 + N + O_2$	1.0e-7
P533	$NO_2^- + O_2^+ N_2 \rightarrow NO_2 + O_2 + N_2$	1.0e-7
P534	$NO_2^- + N_2^+(B^2) \rightarrow NO_2 + N + N$	1.0e-7
P535	$NO_3^- + N_2^+ \rightarrow NO_3 + N + N$	1.0e-7
P536	$NO_3^- + N_3^+ \rightarrow NO_3 + N + N_2$	1.0e-7
P537	$NO_3^- + N_4^+ \rightarrow NO_3 + N_2 + N_2$	1.0e-7
P538	$NO_3^- + O_2^+ \rightarrow NO_3 + O + O$	1.0e-7
P539	$NO_3^- + O_4^+ \rightarrow NO_3 + O_2 + O_2$	1.0e-7
P540	$NO_3^- + NO^+ \rightarrow NO_3 + N + O$	1.0e-7
P541	$NO_3^- + N_2O^+ \rightarrow NO_3 + N_2 + O$	1.0e-7
P542	$NO_3^- + NO_2^+ \rightarrow NO_3 + N + O_2$	1.0e-7
P543	$NO_3^- + O_2^+ N_2 \rightarrow NO_3 + O_2 + N_2$	1.0e-7
P544	$NO_3^- + N_2^+(B^2) \rightarrow NO_3 + N + N$	1.0e-7
P545	$O_4^- + N^+ \rightarrow O_2 + O_2 + N$	1.0e-7
P546	$O_4^- + N_2^+ \rightarrow O_2 + O_2 + N_2$	1.0e-7
P547	$O_4^- + O^+ \rightarrow O_2 + O_2 + O$	1.0e-7
P548	$O_4^- + O_2^+ \rightarrow O_2 + O_2 + O_2$	1.0e-7
P549	$O_4^- + NO^+ \rightarrow O_2 + O_2 + NO$	1.0e-7
P550	$O_4^- + N_2O^+ \rightarrow O_2 + O_2 + N_2O$	1.0e-7
P551	$O_4^- + NO_2^+ \rightarrow O_2 + O_2 + NO_2$	1.0e-7

Table A1. (Continued.)

No.	Reaction	Rate coefficient
P552	$O_4^- + N_3^+ \rightarrow O_2 + O_2 + N_2 + N$	1.0e-7
P553	$O_4^- + N_4^+ \rightarrow O_2 + O_2 + N_2 + N_2$	1.0e-7
P554	$O_4^- + O_4^+ \rightarrow O_2 + O_2 + O_2 + O_2$	1.0e-7
P555	$O_4^- + O_2^+ N_2 \rightarrow O_2 + O_2 + O_2 + N_2$	1.0e-7
P556	$O_4^- + N_2^+(B^2) \rightarrow O_2 + O_2 + N_2$	1.0e-7
P557	$O^- + N^+ + M \rightarrow O + N + M$	2.0e-25* (300.0/TionN) **2.5
P558	$O^- + N_2^+ + M \rightarrow O + N_2 + M$	2.0e-25* (300.0/TionN) **2.5
P559	$O^- + O^+ + M \rightarrow O + O + M$	2.0e-25* (300.0/TionN) **2.5
P560	$O^- + O_2^+ + M \rightarrow O + O_2 + M$	2.0e-25* (300.0/TionN) **2.5
P561	$O^- + NO^+ + M \rightarrow O + NO + M$	2.0e-25* (300.0/TionN) **2.5
P562	$O^- + N_2^+(B^2) + M \rightarrow O + N_2 + M$	2.0e-25* (300.0/TionN) **2.5
P563	$O_2^- + N^+ + M \rightarrow O_2 + N + M$	2.0e-25* (300.0/TionN) **2.5
P564	$O_2^- + N_2^+ + M \rightarrow O_2 + N_2 + M$	2.0e-25* (300.0/TionN) **2.5
P565	$O_2^- + O^+ + M \rightarrow O_2 + O + M$	2.0e-25* (300.0/TionN) **2.5
P566	$O_2^- + O_2^+ + M \rightarrow O_2 + O_2 + M$	2.0e-25* (300.0/TionN) **2.5
P567	$O_2^- + NO^+ + M \rightarrow O_2 + NO + M$	2.0e-25* (300.0/TionN) **2.5
P568	$O_2^- + N_2^+(B^2) + M \rightarrow O_2 + N_2 + M$	2.0e-25* (300.0/TionN) **2.5
P569	$O^- + N^+ + M \rightarrow NO + M$	2.0e-25* (300.0/TionN) **2.5
P570	$O^- + N_2^+ + M \rightarrow N_2O + M$	2.0e-25* (300.0/TionN) **2.5
P571	$O^- + O^+ + M \rightarrow O_2 + M$	2.0e-25* (300.0/TionN) **2.5
P572	$O^- + O_2^+ + M \rightarrow O_3 + M$	2.0e-25* (300.0/TionN) **2.5
P573	$O^- + NO^+ + M \rightarrow NO_2 + M$	2.0e-25* (300.0/TionN) **2.5
P574	$O^- + N_2^+(B^2) + M \rightarrow N_2O + M$	2.0e-25* (300.0/TionN) **2.5
P575	$O_2^- + N^+ + M \rightarrow NO_2 + M$	2.0e-25* (300.0/TionN) **2.5
P576	$O_2^- + O^+ + M \rightarrow O_3 + M$	2.0e-25* (300.0/TionN) **2.5
P577	$O_2^- + NO^+ + M \rightarrow NO_3 + M$	2.0e-25* (300.0/TionN) **2.5
P578	$O_3^- + N^+ + M \rightarrow O_3 + N + M$	2.0e-25* (300.0/TionN2) **2.5
P579	$O_3^- + N_2^+ + M \rightarrow O_3 + N_2 + M$	2.0e-25* (300.0/TionN2) **2.5
P580	$O_3^- + O^+ + M \rightarrow O_3 + O + M$	2.0e-25* (300.0/TionN2) **2.5
P581	$O_3^- + O_2^+ + M \rightarrow O_3 + O_2 + M$	2.0e-25* (300.0/TionN2) **2.5
P582	$O_3^- + NO^+ + M \rightarrow O_3 + NO + M$	2.0e-25* (300.0/TionN2) **2.5
P583	$O_3^- + N_2O^+ + M \rightarrow O_3 + N_2O + M$	2.0e-25* (300.0/TionN2) **2.5
P584	$O_3^- + NO_2^+ + M \rightarrow O_3 + NO_2 + M$	2.0e-25* (300.0/TionN2) **2.5
P585	$O_3^- + N_2^+(B^2) + M \rightarrow O_3 + N_2 + M$	2.0e-25* (300.0/TionN2) **2.5
P586	$NO^- + N^+ + M \rightarrow NO + N + M$	2.0e-25* (300.0/TionN2) **2.5
P587	$NO^- + N_2^+ + M \rightarrow NO + N_2 + M$	2.0e-25* (300.0/TionN2) **2.5
P588	$NO^- + O^+ + M \rightarrow NO + O + M$	2.0e-25* (300.0/TionN2) **2.5
P589	$NO^- + O_2^+ + M \rightarrow NO + O_2 + M$	2.0e-25* (300.0/TionN2) **2.5
P590	$NO^- + NO^+ + M \rightarrow NO + NO + M$	2.0e-25* (300.0/TionN2) **2.5
P591	$NO^- + N_2O^+ + M \rightarrow NO + N_2O + M$	2.0e-25* (300.0/TionN2) **2.5
P592	$NO^- + NO_2^+ + M \rightarrow NO + NO_2 + M$	2.0e-25* (300.0/TionN2) **2.5
P593	$NO^- + N_2^+(B^2) + M \rightarrow NO + N_2 + M$	2.0e-25* (300.0/TionN2) **2.5
P594	$N_2O^- + N^+ + M \rightarrow N_2O + N + M$	2.0e-25* (300.0/TionN2) **2.5
P595	$N_2O^- + N_2^+ + M \rightarrow N_2O + N_2 + M$	2.0e-25* (300.0/TionN2) **2.5
P596	$N_2O^- + O^+ + M \rightarrow N_2O + O + M$	2.0e-25* (300.0/TionN2) **2.5
P597	$N_2O^- + O_2^+ + M \rightarrow N_2O + O_2 + M$	2.0e-25* (300.0/TionN2) **2.5
P598	$N_2O^- + NO^+ + M \rightarrow N_2O + NO + M$	2.0e-25* (300.0/TionN2) **2.5
P599	$N_2O^- + N_2O^+ + M \rightarrow N_2O + N_2O + M$	2.0e-25* (300.0/TionN2) **2.5
P600	$N_2O^- + NO_2^+ + M \rightarrow N_2O + NO_2 + M$	2.0e-25* (300.0/TionN2) **2.5
P601	$N_2O^- + N_2^+(B^2) + M \rightarrow N_2O + N_2 + M$	2.0e-25* (300.0/TionN2) **2.5
P602	$NO_2^- + N^+ + M \rightarrow NO_2 + N + M$	2.0e-25* (300.0/TionN2) **2.5
P603	$NO_2^- + N_2^+ + M \rightarrow NO_2 + N_2 + M$	2.0e-25* (300.0/TionN2) **2.5
P604	$NO_2^- + O^+ + M \rightarrow NO_2 + O + M$	2.0e-25* (300.0/TionN2) **2.5
P605	$NO_2^- + O_2^+ + M \rightarrow NO_2 + O_2 + M$	2.0e-25* (300.0/TionN2) **2.5
P606	$NO_2^- + NO^+ + M \rightarrow NO_2 + NO + M$	2.0e-25* (300.0/TionN2) **2.5
P607	$NO_2^- + N_2O^+ + M \rightarrow NO_2 + N_2O + M$	2.0e-25* (300.0/TionN2) **2.5
P608	$NO_2^- + NO_2^+ + M \rightarrow NO_2 + NO_2 + M$	2.0e-25* (300.0/TionN2) **2.5

Table A1. (Continued.)

No.	Reaction	Rate coefficient
P609	$\text{NO}_2^- + \text{N}_2^+(\text{B}^2) + \text{M} \rightarrow \text{NO}_2 + \text{N}_2 + \text{M}$	$2.0\text{e-}25^*(300.0/\text{TionN2})^{**2.5}$
P610	$\text{NO}_3^- + \text{N}^+ + \text{M} \rightarrow \text{NO}_3 + \text{N} + \text{M}$	$2.0\text{e-}25^*(300.0/\text{TionN2})^{**2.5}$
P611	$\text{NO}_3^- + \text{N}_2^+ + \text{M} \rightarrow \text{NO}_3 + \text{N}_2 + \text{M}$	$2.0\text{e-}25^*(300.0/\text{TionN2})^{**2.5}$
P612	$\text{NO}_3^- + \text{O}^+ + \text{M} \rightarrow \text{NO}_3 + \text{O} + \text{M}$	$2.0\text{e-}25^*(300.0/\text{TionN2})^{**2.5}$
P613	$\text{NO}_3^- + \text{O}_2^+ + \text{M} \rightarrow \text{NO}_3 + \text{O}_2 + \text{M}$	$2.0\text{e-}25^*(300.0/\text{TionN2})^{**2.5}$
P614	$\text{NO}_3^- + \text{NO}^+ + \text{M} \rightarrow \text{NO}_3 + \text{NO} + \text{M}$	$2.0\text{e-}25^*(300.0/\text{TionN2})^{**2.5}$
P615	$\text{NO}_3^- + \text{N}_2\text{O}^+ + \text{M} \rightarrow \text{NO}_3 + \text{N}_2\text{O} + \text{M}$	$2.0\text{e-}25^*(300.0/\text{TionN2})^{**2.5}$
P616	$\text{NO}_3^- + \text{NO}_2^+ + \text{M} \rightarrow \text{NO}_3 + \text{NO}_2 + \text{M}$	$2.0\text{e-}25^*(300.0/\text{TionN2})^{**2.5}$
P617	$\text{NO}_3^- + \text{N}_2^+(\text{B}^2) + \text{M} \rightarrow \text{NO}_3 + \text{N}_2 + \text{M}$	$2.0\text{e-}25^*(300.0/\text{TionN2})^{**2.5}$

are used in the table A1 [134]. Note that T_{gas} is kept at 300 K within this work.

$$\begin{aligned} d\text{Tion} &= 2.0 / (3.0 * 1.3807 \text{e-}16) * 1.6605 \text{e-}24 * (1.0 \text{e-}17 * (\text{E/N}))^{**2} \\ \text{TionN} &= \text{Tgas} + d\text{Tion} * 14.0 * 8.0 \text{e19}^{**2} \\ \text{TionN2} &= \text{Tgas} + d\text{Tion} * 28.0 * 4.1 \text{e19}^{**2} \\ \text{TionN3} &= \text{Tgas} + d\text{Tion} * 42.0 * 6.1 \text{e19}^{**2} \\ \text{TionN4} &= \text{Tgas} + d\text{Tion} * 56.0 * 7.0 \text{e19}^{**2} \\ \text{TeffN} &= (\text{TionN} + 0.5 * \text{Tgas}) / (1.0 + 0.5) \\ \text{TeffN2} &= (\text{TionN2} + 1.0 * \text{Tgas}) / (1.0 + 1.0) \\ \text{TeffN3} &= (\text{TionN3} + 1.5 * \text{Tgas}) / (1.0 + 1.5) \\ \text{TeffN4} &= (\text{TionN4} + 2.0 * \text{Tgas}) / (1.0 + 2.0) \end{aligned}$$

ORCID iDs

Adam Obrusník <https://orcid.org/0000-0002-8415-4909>
 Petr Bílek <https://orcid.org/0000-0002-1579-8751>
 Milan Šimek <https://orcid.org/0000-0003-1730-8493>
 Zdeněk Bonaventura <https://orcid.org/0000-0002-9591-6040>

References

- [1] Šimek M 2014 Optical diagnostics of streamer discharges in atmospheric gases *J. Phys. D: Appl. Phys.* **47** 463001
- [2] Hoder T, Bonaventura Z, Bourdon A and Šimek M 2015 Sub-nanosecond delays of light emitted by streamer in atmospheric pressure air: analysis of $\text{N}_2(\text{C}^3\Pi_u)$ and $\text{N}_2^+(\text{B}^2\Sigma_u^+)$ emissions and fundamental streamer structure *J. Appl. Phys.* **117** 073302
- [3] Kozlov K V, Wagner H E, Brandenburg R and Michel P 2001 Spatio-temporally resolved spectroscopic diagnostics of the barrier discharge in air at atmospheric pressure *J. Phys. D: Appl. Phys.* **34** 3164
- [4] Morrill J *et al* 2002 Electron energy and electric field estimates in sprites derived from ionized and neutral N_2 emissions *Geophys. Res. Lett.* **29** 100-1
- [5] Paris P, Aints M, Valk F, Plank T, Haljaste A, Kozlov K V and Wagner H E 2005 Intensity ratio of spectral bands of nitrogen as a measure of electric field strength in plasmas *J. Phys. D: Appl. Phys.* **38** 3894
- [6] Hoder T, Šimek M, Bonaventura Z, Prukner V and Gordillo-Vázquez F J 2016 Radially and temporally resolved electric field of positive streamers in air and modelling of the induced plasma chemistry *Plasma Sources Sci. Technol.* **25** 045021
- [7] Stepanyan S A, Soloviev V R and Starikovskaya S M 2014 An electric field in nanosecond surface dielectric barrier discharge at different polarities of the high voltage pulse: spectroscopy measurements and numerical modeling *J. Phys. D: Appl. Phys.* **47** 485201
- [8] Gharib M, Mendoza S, Rosenfeld M, Beizai M and Alves Pereira F J 2017 Toroidal plasmoid generation via extreme hydrodynamic shear *Proc. Natl Acad. Sci.* **114** 12657-62
- [9] Zhu X-M and Pu Y-K 2010 Optical emission spectroscopy in low-temperature plasmas containing argon and nitrogen: determination of the electron temperature and density by the line-ratio method *J. Phys. D: Appl. Phys.* **43** 403001
- [10] Gallimberti I, Hepworth J K and Klewe R C 1974 Spectroscopic investigation of impulse corona discharges *J. Phys. D: Appl. Phys.* **7** 880
- [11] Kozlov K V and Wagner H-E 2007 Progress in spectroscopic diagnostics of barrier discharges *Contrib. Plasma Phys.* **47** 26-33
- [12] Hoder T, Loffhagen D, Voráč J, Becker M M and Brandenburg R 2016 Analysis of the electric field development and the relaxation of electron velocity distribution function for nanosecond breakdown in air *Plasma Sources Sci. Technol.* **25** 025017
- [13] Kuo C-L, Hsu R R, Chen A B, Su H T, Lee L-C, Mende S B, Frey H U, Fukunishi H and Takahashi Y 2005 Electric fields and electron energies inferred from the ISUAL recorded sprites *Geophys. Res. Lett.* **32** L19103
- [14] Adachi T, Fukunishi H, Takahashi Y, Hiraki Y, Hsu R-R, Su H-T, Chen A B, Mende S B, Frey H U and Lee L-C 2006 Electric field transition between the diffuse and streamer regions of sprites estimated from ISUAL/array photometer measurements *Geophys. Res. Lett.* **33** L17803
- [15] Kanmae T, Stenbaek-Nielsen H C, McHarg M G and Haaland R K 2010 Observation of sprite streamer head's spectra at 10,000 fps *J. Geophys. Res.: Space Phys.* **115** A00E48
- [16] Celestin S and Pasko V P 2010 Effects of spatial non-uniformity of streamer discharges on spectroscopic diagnostics of peak electric fields in transient luminous events *Geophys. Res. Lett.* **37** L07804
- [17] Naidis G V 2009 Positive and negative streamers in air: Velocity-diameter relation *Phys. Rev. E* **79** 057401
- [18] Bonaventura Z, Bourdon A, Celestin S and Pasko V P 2011 Electric field determination in streamer discharges in air at atmospheric pressure *Plasma Sources Sci. Technol.* **20** 035012
- [19] Ihaddadene M A and Celestin S 2017 Determination of sprite streamers altitude based on N_2 spectroscopic analysis *J. Geophys. Res.: Space Phys.* **122** 1000-14
- [20] Creyghton Y L M 1994 Pulsed positive corona discharges *Fundamental Study and Application to Flue Gas Treatment* Eindhoven University of Technology

- [21] Dyakov A F, Bobrov Y K, Bobrova L N and Yourguelenas Y V 1998 *Physics and Technology of Electric Power Transmission* (Moscow: MPEI)
- [22] Kim Y, Hong S H, Cha M S, Song Y-H and Kim S J 2003 Measurements of electron energy by emission spectroscopy in pulsed corona and dielectric barrier discharges *J. Adv. Oxid. Technol.* **6** 17–22
- [23] Pancheshnyi S 2006 Comments on ‘intensity ratio of spectral bands of nitrogen as a measure of electric field strength in plasmas’ *J. Phys. D: Appl. Phys.* **39** 1708
- [24] Morris M D 1991 Factorial sampling plans for preliminary computational experiments *Technometrics* **33** 161–74
- [25] Capitelli M, Ferreira C M, Gordiets B F and Osipov A I 2000 *Plasma Kinetics in Atmospheric Gases* (Springer Series on Atomic, Optical, and Plasma Physics) (Berlin: Springer)
- [26] Kossyi I A, Kostinsky A Y, Matveyev A A and Silakov V P 1992 Kinetic scheme of the non-equilibrium discharge in nitrogen–oxygen mixtures *Plasma Sources Sci. Technol.* **1** 207
- [27] Gordiets B F, Ferreira C M, Guerra V L, Loureiro J M A H, Nahorny J, Pagnon D, Touzeau M and Vialle M 1995 Kinetic model of a low-pressure N₂–O₂ flowing glow discharge *IEEE Trans. Plasma Sci.* **23** 750–68
- [28] Flitti A and Pancheshnyi S 2009 Gas heating in fast pulsed discharges in N₂–O₂ mixtures *Eur. Phys. J. Appl. Phys.* **45** 21001
- [29] Pancheshnyi S, Eismann B, Hagelaar G J M and Pitchford L C 2008 Computer code ZDPlasKin 11th Int. Symp. on High Pressure, Low Temperature Plasma Chemistry
- [30] Hairer E and Wanner G 1996 Solving ordinary differential equations: II Stiff and Differential-Algebraic Problems 2nd edn (Berlin: Springer)
- [31] Hagelaar G J M and Pitchford L C 2005 Solving the Boltzmann equation to obtain electron transport coefficients and rate coefficients for fluid models *Plasma Sources Sci. Technol.* **14** 722
- [32] LXcat, Biagi database (Accessed: 20 June 2017) www.lxcat.net
- [33] MAGBOLTZ, Magboltz, Fortran program, MAGBOLTZ, S. F. Biagi, versions 8.9 and after magboltz.web.cern.ch
- [34] LXcat, Phelps database (Accessed: 20 June 2017) www.lxcat.net
- [35] A V Phelps, A V Phelps, jilawww.colorado.edu/~avp/
- [36] LXcat, TRINITI database (Retrieved: 20 June 2017) www.lxcat.net
- [37] LXcat, IST-lisbon database (Retrieved: 20 June 2017) www.lxcat.net
- [38] Alves L L and Alves L L 2014 The IST-Lisbon database on LXCat *J. Phys.: Conf. Ser.* **565** 1
- [39] Soboł I M 2001 *Mathematics and Computers in Simulation* **55** 271–80
- [40] Turányi T 1990 Sensitivity analysis of complex kinetic systems. tools and applications *J. Math. Chem.* **5** 203–48
- [41] Turányi T 1997 Applications of sensitivity analysis to combustion chemistry *Reliab. Eng. Syst. Saf.* **57** 41–8 The Role of Sensitivity Analysis in the Corroboration of Models and its Links to Model Structural and Parametric Uncertainty
- [42] Mazánková V, Trunec D and Krčma F 2014 Study of nitrogen flowing afterglow with mercury vapor injection *J. Chem. Phys.* **141** 154307
- [43] Mazánková V, Trunec D, Navrátil Z, Raud J and Krčma F 2016 Study of argon–oxygen flowing afterglow *Plasma Sources Sci. Technol.* **25** 035008
- [44] Turner M M 2015 Uncertainty and error in complex plasma chemistry models *Plasma Sources Sci. Technol.* **24** 035027
- [45] Campolongo F, Cariboni J and Saltelli A 2007 An effective screening design for sensitivity analysis of large models *Environ. Modelling Softw.* **22** 1509–18
- [46] Paris P, Aints M, Laan M and Valk F 2004 Measurement of intensity ratio of nitrogen bands as a function of field strength *J. Phys. D: Appl. Phys.* **37** 1179
- [47] Paris P, Aints M, Valk F, Plank T, Haljaste A, Kozlov K V and Wagner H E 2006 Reply to comments on ‘intensity ratio of spectral bands of nitrogen as a measure of electric field strength in plasmas’ *J. Phys. D: Appl. Phys.* **39** 2636
- [48] Hoder T, Brandenburg R, Basner R, Weltmann K-D, Kozlov K V and Wagner H-E 2010 A comparative study of three different types of barrier discharges in air at atmospheric pressure by cross-correlation spectroscopy *J. Phys. D: Appl. Phys.* **43** 124009
- [49] McConkey J W and Latimer I D 1965 Absolute cross sections for simultaneous ionization and excitation of N₂ by electron impact *Proc. Phys. Soc.* **86** 463
- [50] Stanton P N and John R M St 1969 Electron excitation of the first positive bands of N₂ and of the first negative and Meinel bands of N₂⁺ *J. Opt. Soc. Am.* **59** 252–60
- [51] Borst W L and Zipf E C 1970 Cross section for electron-impact excitation of the (0, 0) first negative band of N₂⁺ from threshold to 3 keV *Phys. Rev. A* **1** 834
- [52] McConkey J W, Woolsey J M and Burns D J 1967 Absolute cross section for electron impact excitation of 3914 Å N₂⁺ *Planet. Space Sci.* **15** 1332–4
- [53] McConkey J W, Woolsey J M and Burns D J 1971 Absolute cross section for electron impact excitation of 3914 Å N₂⁺ *Planet. Space Sci.* **19** 1192
- [54] Skubenich V V and Zapesochny I P 1981 Excitation of molecular ion states upon collision of monoenergetic electrons with atmospheric gas molecules no.1 N₂⁺ (spectral bands) *Geomagn. Aeronomy* **21** 355–60
- [55] Itikawa Y 2006 Cross sections for electron collisions with nitrogen molecules *J. Phys. Chem. Ref. Data* **35** 31–53
- [56] Tohyama Y and Nagata T 2011 Absolute and relative measurements of optical emission cross sections for the N₂⁺ 1N(v', v'') bands by electron impact *J. Phys. Soc. Japan* **80** 034304
- [57] Jobe J D, Sharpton F A and John R M St 1967 Apparent cross sections of N₂ for electron excitation of the second positive system *J. Opt. Soc. Am.* **57** 106–7
- [58] Burns D J, Simpson F R and McConkey J W 1969 Absolute cross sections for electron excitation of the second positive bands of nitrogen *J. Phys. B: At. Mol. Phys.* **2** 52
- [59] Aarts J F M and De Heer F J 1969 Emission cross sections of the second positive group of nitrogen produced by electron impact *Chem. Phys. Lett.* **4** 116–8
- [60] Shemansky D E and Broadfoot A L 1971 Excitation of N₂ and N₂⁺ systems by electronsii. excitation cross sections and N₂1PG low pressure afterglow *J. Quant. Spectrosc. Radiat. Transfer* **11** 1401–39
- [61] Imami M and Borst W L 1974 Electron excitation of the (0, 0) second positive band of nitrogen from threshold to 1000 eV *J. Chem. Phys.* **61** 1115–7
- [62] Shemansky D E, Ajello J M and Kanik I 1995 Electron excitation function of the N₂ second positive system *Astrophys. J.* **452** 472
- [63] Fons J T, Schpe R S and Lin C C 1996 Electron-impact excitation of the second positive band system (C³Π_u → B³Π_g) and the C³Π_u electronic state of the nitrogen molecule *Phys. Rev. A* **53** 2239
- [64] Tohyama Y and Nagata T 2005 Electron impact emission of N₂ 2P(v', v'') bands studied under single-collision condition *J. Phys. Soc. Japan* **74** 326–32
- [65] Malone C P, Johnson P V, Young J A, Liu X, Ajdari B, Khakoo M A and Kanik I 2009 Integral cross sections for electron-impact excitation of the C³Π_u, E³Σ_g⁺ and a''/l^{Σ_g⁺ states of N₂ *J. Phys. B: At. Mol. Opt. Phys.* **42** 225202}
- [66] Šimek M 2002 The modelling of streamer-induced emission in atmospheric pressure, pulsed positive corona discharge:

- N₂ second positive and NO- γ systems *J. Phys. D: Appl. Phys.* **35** 1967
- [67] Bennett R G and Dalby F W 1959 Experimental determination of the oscillator strength of the first negative bands of N₂⁺ *J. Chem. Phys.* **31** 434–41
- [68] Fink E and Welge K H 1964 Lebensdauer der elektronenzustände N₂(C³Π_u), N₂⁺(B²Σ_u⁺), NH(A³Π), NH(c¹Π), PH(³Π) *Z. Naturforsch. A* **19** 1193–201
- [69] Sebacher D I 1965 Study of collision effects between the constituents of a mixture of helium and nitrogen gases when excited by a 10-keV electron beam *J. Chem. Phys.* **42** 1368–72
- [70] Jeunehomme M 1966 Oscillator strengths of the first negative and second positive systems of nitrogen *J. Chem. Phys.* **44** 2672–7
- [71] Fowler R G and Holzberlein T M 1966 Transition probabilities for H₂, D₂, N₂, N₂⁺, and CO *J. Chem. Phys.* **45** 1123–5
- [72] Hesser J E 1968 Absolute transition probabilities in ultraviolet molecular spectra *J. Chem. Phys.* **48** 2518–35
- [73] Nichols L L and Wilson W E 1968 Optical lifetime measurements using a positive ion van de graaff accelerator *Appl. Opt.* **7** 167–70
- [74] Desesquelles J, Dufay M and Poulizac M C 1968 Lifetime measurement of molecular states with an accelerated ion beam *Phys. Lett. A* **27** 96–7
- [75] Johnson A W and Fowler R G 1970 Measured lifetimes of rotational and vibrational levels of electronic states of N₂ *J. Chem. Phys.* **53** 65–72
- [76] Sawada T and Kamada H 1970 Radiative lifetime measurements of some excited states of N₂⁺ and CH *Bull. Chem. Soc. Japan* **43** 325–30
- [77] Head C E 1971 Radiative lifetimes of the B²Σ_u⁺ ν' = 0 and ν' = 1 levels of N₂⁺ *Phys. Lett. A* **34** 92–3
- [78] Dotchin L W, Chupp E L and Pegg D J 1973 Radiative lifetimes and pressure dependence of the relaxation rates of some vibronic levels in N₂⁺, N₂, CO⁺, and CO *J. Chem. Phys.* **59** 3960–7
- [79] Dufayard J, Negre J M and Nedelec O 1974 Perturbation effects on lifetimes in N₂⁺ *J. Chem. Phys.* **61** 3614–8
- [80] Erman P 1975 High resolution measurements of atomic and molecular lifetimes using the high frequency deflection technique *Phys. Scr.* **11** 65
- [81] Smith A J, Read F H and Imhof R E 1975 Measurement of the lifetimes of ionic excited states using the inelastic electron-photon delayed coincidence technique *J. Phys. B: At. Mol. Phys.* **8** 2869
- [82] Chen C H, Payne M G, Hurst G S and Judish J P 1976 Kinetic studies of N₂ and N₂-SF₆ following proton excitation *J. Chem. Phys.* **65** 3863–8
- [83] Remy F and Dumont M N 1978 The radiative lifetime of the B²Σ_u⁺ state of N₂⁺: a new measurement and a discussion of previous results *J. Quant. Spectrosc. Radiat. Transfer* **20** 217–22
- [84] Jolly J and Plain A 1983 Determination of the quenching rates of N₂⁺(B²Σ_u⁺, ν = 0, 1) by N₂ using laser-induced fluorescence *Chem. Phys. Lett.* **100** 425–8
- [85] Plain A and Jolly J 1984 Quenching rate constants for N₂⁺(B²Σ_u⁺, ν' = 0, 1, 2) with N₂ and Ne *Chem. Phys. Lett.* **111** 133–5
- [86] Wuerker R F, Schmitz L, Fukuchi T and Straus P 1988 Lifetime measurements of the excited states of N₂ and N₂⁺ by laser-induced fluorescence *Chem. Phys. Lett.* **150** 443–6
- [87] Langhoff S R and Bauschlicher C W Jr 1988 Theoretical study of the first and second negative systems of N₂⁺ *J. Chem. Phys.* **88** 329–36
- [88] Schmoranz H, Hartmetz P, Marger D and Dudda J 1989 Lifetime measurement of the B²Σ_u⁺ (ν = 0) state of ¹⁴N₂⁺ by the beam-dye-laser method *J. Phys. B: At. Mol. Opt. Phys.* **22** 1761
- [89] Gilmore F R, Laher R R and Espy P J 1992 Frank-condon factors, r-centroids, electronic transition moments, and einstein coefficients for many nitrogen and oxygen band system *J. Phys. Chem. Ref. Data* **21** 1005–107
- [90] Fukuchi T, Wong A Y and Wuerker R F 1995 Lifetime measurement of the B²Σ_u⁺ level of N₂⁺ by laser-induced fluorescence *J. Appl. Phys.* **77** 4899–902
- [91] Pancheshnyi S V, Starikovskiaia S M and Starikovskii A Y 1998 Measurements of rate constants of the N₂(C³Π_u, ν = 0) and N₂⁺(B²Σ_u⁺, ν = 0) deactivation by N₂, O₂, H₂, CO and H₂O molecules in afterglow of the nanosecond discharge *Chem. Phys. Lett.* **294** 523–7
- [92] Rosado J, Blanco F, Arqueró F and Ortiz M 2008 Measurements of air fluorescence induced by low-energy electrons at low pressures *Nucl. Instrum. Methods Phys. Res. A* **597** 83–7
- [93] Dilecce G, Ambrico P F and De Benedictis S 2010 On the collision quenching of by N₂ and O₂ and its influence on the measurement of E/N by intensity ratio of nitrogen spectral bands *J. Phys. D: Appl. Phys.* **43** 195201
- [94] Anton H 1966 Zur lumineszenz einiger molekülgase bei anregung durch schnelle elektronen: II *Ann. Phys., Lpz.* **473** 178–93
- [95] Sawada T and Kamada H 1970 Radiative lifetime measurements of N₂(C³Π_u), NH(A³Π) and NH(C¹Π) *Bull. Chem. Soc. Japan* **43** 331–4
- [96] Calo J M and Axtmann R C 1971 Vibrational relaxation and electronic quenching of the C³Π u (v' = 1) state of nitrogen *J. Chem. Phys.* **54** 1332–41
- [97] Imhof R E and Read F H 1971 Measured lifetimes of the C³Π_u state of N₂ and the a³Σ_g⁺ state of H₂ *J. Phys. B: At. Mol. Phys.* **4** 1063
- [98] Millet P, Salamero Y, Brunet H, Galy J, Blanc D and Teyssier J L 1973 De-excitation of N₂(C³Π_u; ν = 0 and 1) levels in mixtures of oxygen and nitrogen *J. Chem. Phys.* **58** 5839–41
- [99] Becker K H, Engels H and Tatarczyk T 1977 Lifetime measurements of the C³Π_u state of nitrogen by laser-induced fluorescence *Chem. Phys. Lett.* **51** 111–5
- [100] Carr T W and Dondes S 1977 Direct measurement of the radiative lifetime and collisional quenching of the C³Π_u state of nitrogen as studied by pulse radiolysis *J. Phys. Chem.* **81** 2225–8
- [101] Bennett W R Jr and Flint J 1978 Ar(²P₃)–N₂ C³Π_u excitation transfer cross section and radiative lifetimes of the nitrogen-molecular-laser transitions *Phys. Rev. A* **18** 2527
- [102] Larsson M and Radozycki T 1982 Time resolved studies of perturbations in the ν' = 1 level and radiative properties of the C³Π_u state in N₂ *Phys. Scr.* **25** 627
- [103] Dumont M N and Remy F 1982 The radiative lifetime of the C³Π_u state of N₂ *J. Chem. Phys.* **76** 1175–6
- [104] Werner H-J, Kalcher J and Reinsch E-A 1984 Accurate *ab initio* calculations of radiative transition probabilities between the A³σg_u⁺, B³Π_g, W³Δ_u, B³Σ_u, and C³Π_u states of N₂ *J. Chem. Phys.* **81** 2420–31
- [105] Fukuchi T, Wuerker R F and Wong A Y 1992 Lifetime and transition probability measurements of the second positive system of nitrogen by laser-induced fluorescence *J. Chem. Phys.* **97** 9490–1
- [106] Erman P 1993 Elusive C³Π_u state lifetime of molecular nitrogen *Phys. Rev. A* **48** R3421
- [107] Simon M D, Wuerker R F and Wong A Y 1994 Measurement of the C³Π_u radiative lifetime of N₂ by laser-induced fluorescence *Phys. Rev. A* **50** 2978
- [108] Dilecce G, Ambrico P F and De Benedictis S 2007 On N₂(C³Π_u, ν = 0) state lifetime and collisional deactivation rate by N₂ *Chem. Phys. Lett.* **444** 39–43
- [109] Hirsh M N, Halpern G M, Slevin J A and Wolf N S 1966 Ionization and electron loss simulation in atmospheric gases *Technical Report DEWEY (GC) CORP*, New York

- [110] Brocklehurst B and Downing F A 1967 Mechanisms of excitation of luminescence in nitrogen gas by fast electrons *J. Chem. Phys.* **46** 2976–91
- [111] Comes E J and Speier F 1969 The optical formation and the collisional deactivation of the first negative system of nitrogen *Chem. Phys. Lett.* **4** 13–6
- [112] Mitchell K B 1970 Fluorescence efficiencies and collisional deactivation rates for N₂ and N₂⁺ bands excited by soft X rays *J. Chem. Phys.* **53** 1795–802
- [113] Hirsh M N, Poss E and Eisner P N 1970 Absolute fluorescence yields of 3914-Å photons from N₂ and air excited by relativistic electrons *Phys. Rev. A* **1** 1615
- [114] Mackay G I and March R E 1971 Collisional deactivation rates of N₂^{+(B²Σ_u⁺) *Can. J. Chem.* **49** 1268–71}
- [115] Tellinghuisen J B, Winkler C A, Freeman C G, McEwan M J and Phillips L F 1972 Quenching rates for N₂⁺, N₂O⁺, and CO₂⁺ emission bands excited by 58.4 nm irradiation of N₂, N₂O, and CO₂ *J. Chem. Soc. Faraday Trans. II* **68** 833–8
- [116] Beikov A E, Kusnetsov O V and Sharafutdinov R G 1995 The rate of collisional quenching of N₂O^{+(B²Σ), N₂^{+(B²Σ), O₂^{+(b⁴Σ), O^{+(3d), O(3p), Ar^{+(4p'), Ar(4p,4p') at the temperature ≤ 200 K *J. Chem. Phys.* **102** 2792–801}}}}}
- [117] Waldenmaier T, Blümer J, Gonzalez D M and Klages H 2008 Measurement of the air fluorescence yield with the airlight experiment *Nucl. Instrum. Methods Phys. Res. A* **597** 67–74
- [118] Valk F, Aints M, Paris P, Plank T, Maksimov J and Tamm A 2010 Measurement of collisional quenching rate of nitrogen states N₂(C³Π_u, v = 0) and N₂^{+(B²Σ_u⁺, v = 0) *J. Phys. D: Appl. Phys.* **43** 385202}
- [119] Albugues F, Birot A, Blanc D, Brunet H, Galy J, Millet P and Teyssier J L 1974 Destruction of the levels C³Π_u ($\nu' = 0$, $\nu' = 1$) of nitrogen by O₂, CO₂, CH₄, and H₂O *J. Chem. Phys.* **61** 2695–9
- [120] Pancheshnyi S V, Starikovskaya S M and Starikovskii A Y 2000 Collisional deactivation of N₂(C³Π_u, v = 0, 1, 2, 3) states by N₂, O₂, H₂ and H₂O molecules *Chem. Phys.* **262** 349–57
- [121] Erman P 2001 Comment on measurements of the collisional deactivation rate of the C³Π_u state *Chem. Phys. Lett.* **342** 515–8
- [122] Dilecce G, Ambriaco P F and Benedictis S De 2006 OODR-LIF direct measurement of N₂(C³Π_u, v = 0–4) electronic quenching and vibrational relaxation rate coefficients by N₂ collision *Chem. Phys. Lett.* **431** 241–6
- [123] Morozov A, Heindl T, Wieser J, Krücke R and Ulrich A 2008 Influence of pressure on the relative population of the two lowest vibrational levels of the C³Π_u state of nitrogen for electron beam excitation *Eur. Phys. J. D* **46** 51–7
- [124] Pereira L, Morozov A, Fraga M M, Heindl T, Krücke R, Wieser J and Ulrich A 2010 Temperature dependence of the quenching of N₂ C³Π_u by N₂(X) and O₂(X) *Eur. Phys. J. D* **56** 325–34
- [125] Warneck P 1967 Studies of ionneutral reactions by a photoionization mass-spectrometer technique: I *J. Chem. Phys.* **46** 502–12
- [126] McKnight L G, McAfee K B and Sipler D P 1967 Low-field drift velocities and reactions of nitrogen ions in nitrogen *Phys. Rev.* **164** 62
- [127] Moseley J T, Snuggs R M, Martin D W and McDaniel E W 1969 Mobilities, diffusion coefficients, and reaction rates of mass-indentified nitrogen ions in nitrogen *Phys. Rev.* **178** 240
- [128] Good A, Durden D A and Kebarle P 1970 Ion-molecule reactions in pure nitrogen and nitrogen containing traces of water at total pressures 0.5–4 Torr. kinetics of clustering reactions forming H^{+(H₂O)_n *J. Chem. Phys.* **52** 212–21}
- [129] Böhringer H and Arnold F 1982 Temperature dependence of three-body association reactions from 45 to 400 K. the reactions N₂⁺ + 2N₂ \longrightarrow N₄⁺ + N₂ and O₂⁺ + 2O₂ \longrightarrow O₄⁺ + O₂ *J. Chem. Phys.* **77** 5534–41
- [130] Sieck L W, Heron J T and Green D S 2000 Chemical kinetics database and predictive schemes for humid air plasma chemistry: I. Positive ion-molecule reactions *Plasma Chem. Plasma Process.* **20** 235–58
- [131] Frost M J and Sharpe C R J 2001 Time-resolved kinetic studies of the N₂⁺ + N₂ association reaction *Phys. Chem. Chem. Phys.* **3** 4536–41
- [132] Troe J 2005 Temperature and pressure dependence of ion-molecule association and dissociation reactions: the N₂⁺ + N₂ (+M) \longleftrightarrow N₄⁺ (+M) reaction *Phys. Chem. Chem. Phys.* **7** 1560–7
- [133] Hagelaar G J M and Pitchford L C 2005 Solving the Boltzmann equation to obtain electron transport coefficients and rate coefficients for fluid models *Plasma Sources Sci. Technol.* **14** 722
- [134] McKnight L G, McAfee K B and Sipler D P 1967 Low-field drift velocities and reactions of nitrogen ions in nitrogen *Phys. Rev.* **164** 62–70